AD NUMBER

AD161563

NEW LIMITATION CHANGE

TO

Approved for public release, distribution unlimited

FROM

No Foreign

AUTHORITY

ONR ltr., 26 Oct 77

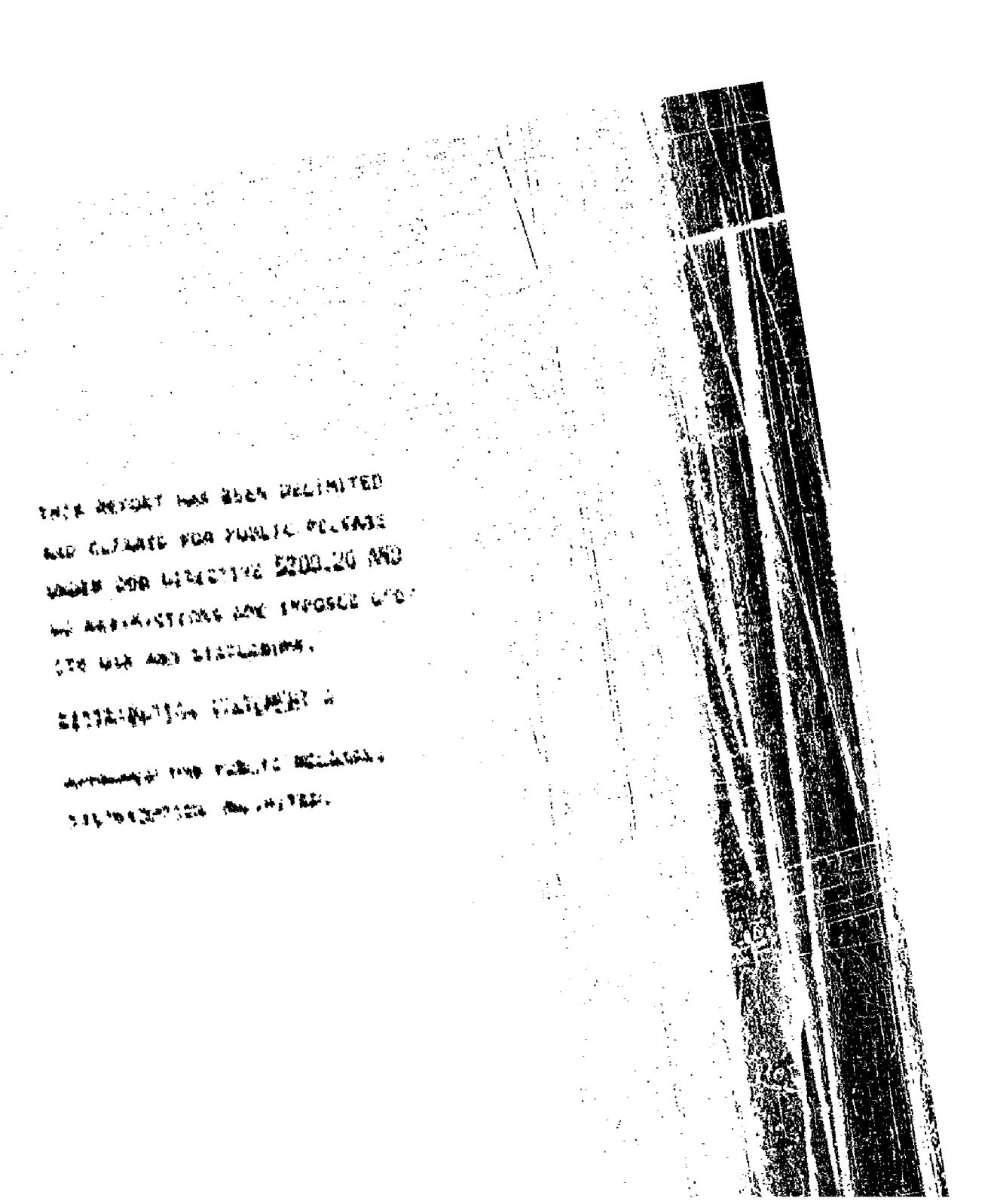

(6)

Report Number
I 58-1

An Experimental Investigation of High Frequency Combustion Pressure Oscillations in a Gaseous Bipropellant Rocket Motor

R. Osborn and R.M. Schiewe

Contract N7 onr 39418

June 1958

JET PROPULSION CENTER
PURDUE UNIVERSITY
SCHOOL OF MECHANICAL ENGINEERING
LAFAYETTE, INDIANA

Purdue University
and
Purdue Research Foundation
Lafayette, Indiana

Report No. I-58-1

AN EXPERIMENTAL INVESTIGATION OF HIGH FREQUENCY COMBUSTION PRESSURE OSCILLATIONS IN A GASEOUS BIPROPELLANT ROCKET MOTOR

by
J. R. Osborn and R. M. Schiewe

Interim Report No. 1-58-1
Contract N7 onr 39418

Jet Propulsion Center
Purdue University

June 1958

ACKNOWLEDGMENTS

The authors wish to express their gratitude to Dr. M. J. Zucrow, Professor of Gas Turbines and Jet Propulsion, Purdue University, for his helpful guidance throughout the course of the investigation. The authors are also grateful to Drs. C. F. Warner and B. A. Reese for their administration of the project, to Mr. A. C. Pinchak for his helpful assistance in conducting part of the investigation, and to all other personnel of the Purdue Jet Propulsion Center.

Acknowledgment is also given to the Office of Naval Research, Contract N7 onr-39418, under whose sponsorship the research reported herein was conducted. Reproduction in full or in part is permitted for any use of the United States Government.

TABLE OF CONTENTS

LIST OF ILLUSTRATIONS

LIST OF ILLUSTRATIONS (Continued)

LIST OF TABLES

ABSTRACT

An experimental investigation was conducted that was concerned with the initial phases of a research program for determining the manner in which certain basic variables influence the high frequency combustion pressure oscillations in a rocket motor. The experimental investigation reported herein was conducted with a gaseous bipropellant rocket motor which simplified the experimental work by eliminating several variables which enter into the combustion process: atomization, vaporization, mixing, etc.

The combustion pressure oscillations observed in the subject investigation had frequencies ranging from 550 to 1725 cycles per second for a transverse mode. The combustion pressure oscillations were measured with a cathode ray oscillograph.

The effects of combustion chamber geometry, the nozzle configuration, the heat-release rates of the propellants, the combustion pressure, and the equivalence ratio upon the combustion pressure oscillations were investigated.

It is planned to continue the experimental work performed with the gaseous bipropellant rocket motor so that additional basic information regarding the mechanism of high frequency combustion pressure oscillations can be determined.

INTRODUCTION

In general, there are two basic types of combustion pressure oscillations encountered in rocket motors; "low frequency combustion pressure oscillations" and "high frequency combustion pressure oscillations." This report will be concerned only with the high frequency combustion pressure oscillations (1)(2).*

The frequency range of high frequency combustion pressure oscillations may be from several hundred cycles per second to possibly 12,000 cycles per second, and the mode of oscillation may be longitudinal, radial, or tangential (see Fig. 1). It is believed that the tangential mode, also called the "sloshing" mode, is the most destructive to the rocket motor. From a broad point of view it is possible to segregate the variables influencing the combustion mechanism of liquid propellants into three classes discussed below. Although the pertinent variables are listed separately for simplicity, it is recognized that all of them are interrelated and many of them act simultaneously. The afore-mentioned three classes of variables are

(1) variables pertinent to the preparation of the propellant for combustion;

(2) variables which influence the reaction kinetics of the mixture, including those influencing the rate of heat transfer to the mixture; and

---

* Numbers in parentheses apply to references in the Bibliography, Appendix E.

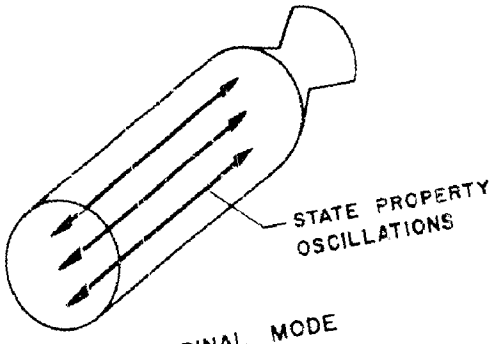

(a) LONGITUDINAL MODE

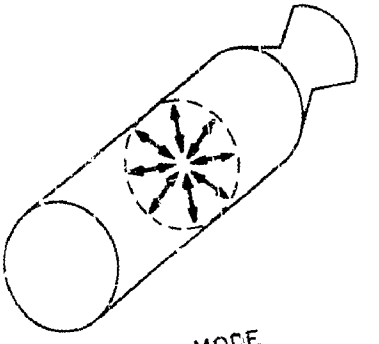

(b) RADIAL MODE

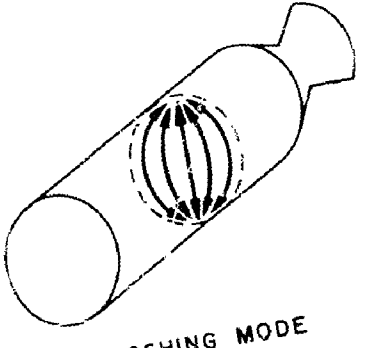

(c) SLOSHING MODE

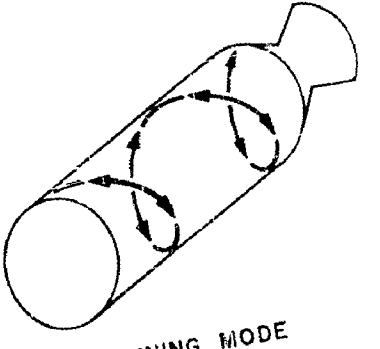

(d) SPINNING MODE

Fig. 1 Modes of Oscillation

(3) variables related to the geometric configuration of the thrust chamber and the exhaust nozzle, which influence the gas dynamical processes in the rocket motor.

Variables Which May Influence Combustion Pressure Oscillations

The individual variables, which may play a part in either aggravating or dampening the tendency for high frequency combustion pressure oscillations to occur, will be listed as three separate groups.

(a) Propellant Preparation Factors. The principal variables related to the preparation of the propellants for combustion are as follows:

(1) the degree of atomization of the propellants;

(2) the penetration of the propellant streams into the gases existing in the combustion chamber;

(3) the vaporization rate of the propellants;

(4) the degree of uniformity of the vaporized propellants (reactive mixture);

(5) the temperature distribution of the reactive mixture;

(6) the spatial distribution of the reactive mixture in the thrust chamber; and

(7) the fuel/oxidizer ratio distribution for the reactive mixture.

(b) Chemical and Heat Transfer Factors. This category includes the following:

(1) the rate of flame propagation through the pertinent propellants at different mixture ratios;

(2) the effect of the temperature and pressure of the vaporized propellants upon the rate of burning at different mixture ratios;

(3) the effect of non-uniformity in the mixture distribution upon the burning rates;

(4) the effect of the temperature distribution upon the burning rates;

(5) the effect of diluents, such as the hot burned gases which are recirculated into the vaporized propellants, upon the temperature distribution, homogeneity, and burning rates.

(c) Geometrical Factors. The geometrical factors which appear to be important are as follows:

(1) the aspect ratio which may influence the recirculation of hot gases and the reflection of pressure waves to the combustible mixture;

(2) the configuration of the exhaust nozzle, since it too may influence the recirculation of hot gases and the reflection of pressure waves into the combustible mixture; and

(3) the combustion volume, especially with respect to the effect of different distributions of the propellant mixture upon the combustion processes.

Scope of the Research Program

The objectives of the research program are concerned with determining the relative importance of several of the pertinent physical and chemical factors upon combustion pressure oscillations. Because of the great experimental difficulties attendant upon the determination of the influence of each of the pertinent variables separately and in the interest of simplifying the experimental work it was deemed logical to eliminate as many of the variables as possible, especially in conducting the

first phases of the research program. Consequently, first phases of the research program were concerned with the factors influencing the oscillations in the combustion pressure of a rocket motor burning a gaseous oxidizer and a gaseous fuel.

The principal reasons for conducting the initial investigations with a gaseous bipropellant rocket motor are as follows:

(1) any influence of the vaporization of the propellants is thus eliminated;

(2) the mixing of the gaseous oxidizer and gaseous fuel can be readily controlled;

(3) the heat-release rate of the propellants can be changed markedly and conveniently by merely changing the gas used for the fuel, or the gas used as the oxidizer;

(4) the effect of diluents, such as nitrogen or carbon dioxide, can be studied conveniently;

(5) the non-homogeneity in the composition of the reactive mixture can be controlled quite readily; and

(6) the fuel/oxidizer ratio can be readily changed, and even varied throughout the rocket motor.

Details of the Research Program

Below is presented the detailed research program, which is of necessity a long range program, and divided into six phases.

Phase I. This phase is concerned with studies for determining the effect of the pertinent variables upon the combustion pressure oscillations in a gaseous bipropellant rocket motor for a single bipropellant combination.

Phase II. This phase is concerned with studies for determining the effect of the heat-release rates of the propellant upon the combustion pressure oscillations.

Phase III. This phase is to be concerned with studying the effect of the vaporization characteristics of different oxidizers; the fuel being in the gaseous state.

Phase IV. This phase will be concerned with studies of the effect of the vaporization characteristics of different fuels; the oxidizer being in the gaseous state.

Phase V. In this phase the experimental results obtained from Phases I and IV inclusive will be correlated with the object of developing a theory which can be applied by the designer of a rocket motor.

Phase VI. This phase comprises an experimental program for checking the theoretical results developed under Phase V.

The present report is concerned with the results of experimental investigations conducted under Phases I and II above. The investigations were conducted for the purpose of determining the influences of the following variables upon the frequency and amplitude of high frequency combustion pressure oscillations in a gaseous bipropellant rocket motor; (1) combustion chamber length, (2) steady state combustion pressure, and (3) the configurations of the exhaust nozzle.

METHOD OF INVESTIGATION

General Procedure

1. Investigation of the Effect of Combustion Chamber Length

In these experiments the length of the combustion chamber L was changed, in steps, from 6 in. to 16 in. by inserting or removing spacing rings as required. A series of experiments with L as the variable was conducted with each of the following propellant combinations; (a) methane-air, (b) ethane-air, (c) ethylene-air, and (d) propane-air. In each series of experiments the other pertinent variables, such as steady-state combustion pressure, pressure drops in the air and fuel lines, the nozzle configuration, the injector configuration, fuel-air premixing chamber configurations, and equivalence ratio were maintained constant.*

The combustion pressure oscillations were measured with Photocon pressure transducers in conjunction with a six-channel Hathaway cathode ray oscillograph (See Appendix B). Figure 2 illustrates schematically the locations of the pressure transducers; at least two were located 2 1/2 inches downstream from the face of the injector and one 2 1/2 inches upstream from the entrance plane of the exhaust nozzle.

In all of the experiments discussed in this report, the variables for computing the air and fuel (gas) flow rates, were measured, and

---

* Equivalence ratio is the fuel-air ratio (by weight) divided by the stoichiometric fuel-air ratio.

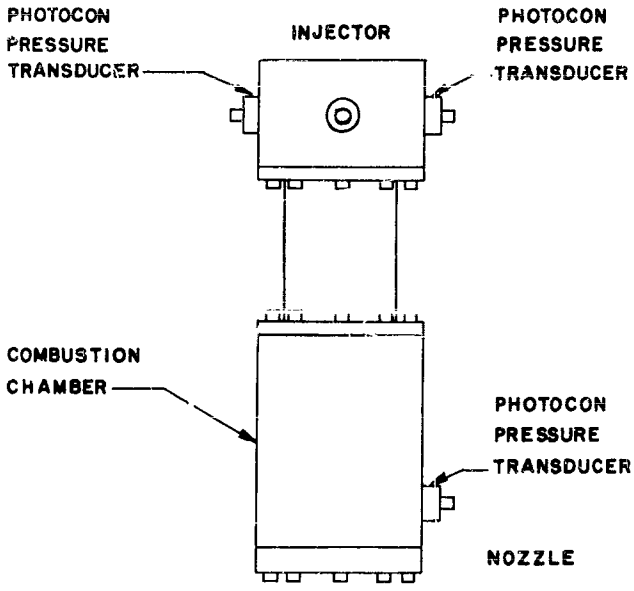

Fig.2 Location of the High Frequency Pressure Transducers in the Combustion Chamber

also the injection and steady-state combustion pressures.

Figure 3 is a schematic flow diagram for the apparatus employed in all of the experiments discussed in this report. The detailed operating procedure is described in Appendix C.

2. Investigation of Effect of Steady-State Combustion Pressure and Equivalence Ratio

In these experiments the equivalence ratio was varied from the rich to the lean limits of inflammability, for different constant values of steady-state combustion pressure. The latter was varied from 20 to 200 psia. The experiments were conducted with methane and air, ethane and air, and ethylene and air. In all cases such variables as the length of combustion chamber, the mixing chamber configuration, injector configuration, and nozzle configuration were held constant.

The oscillations in the combustion pressure were measured with four Photocon pressure transducers in conjunction with a six-channel cathode ray oscillograph. Three of the pressure transducers were spaced circumferentially (90° apart) 2 1/2 inches downstream from the injector and the fourth was located 2 1/2 inches upstream from the nozzle (see Fig. 2).

3. Investigation of Influence of Nozzle Configuration

In this series of experiments three different converging nozzles were employed; their geometry is illustrated in Fig. 4. In all cases the propellants were methane and air.

Each nozzle was operated with the following parameters maintained constant; the pressure drops in the air and methane supply lines, the mixture chamber configuration, the injector configuration, the equivalence

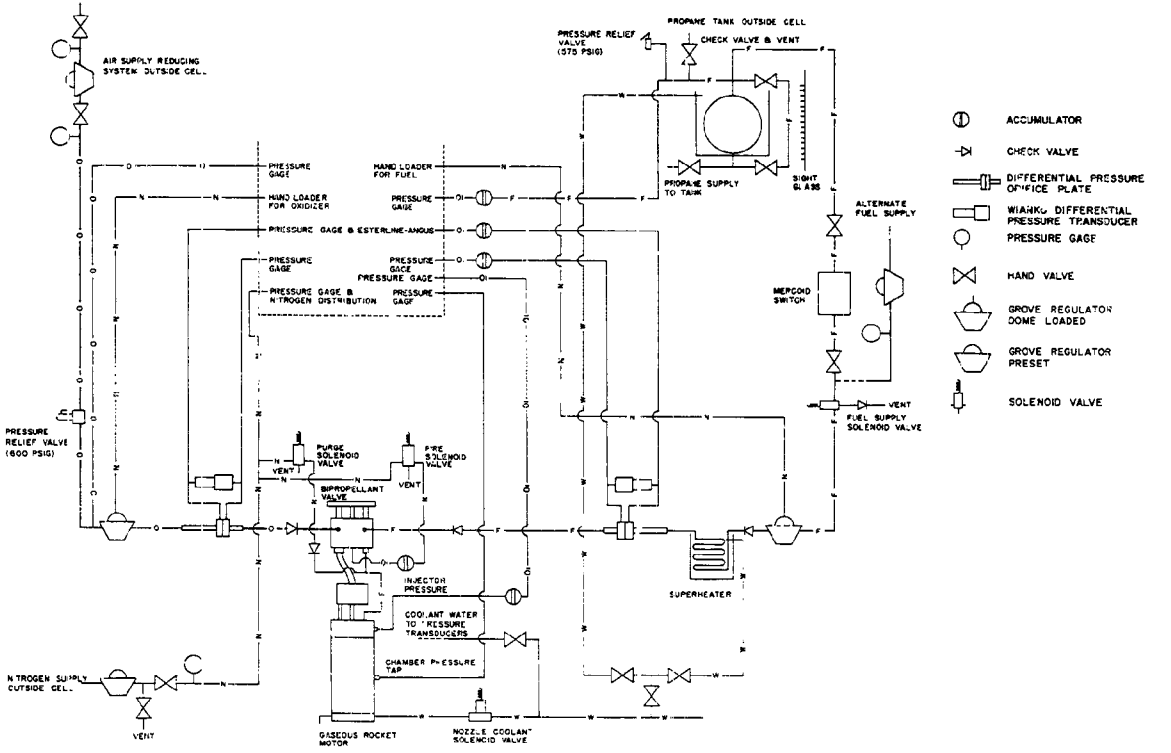

Fig. 3 Schematic Diagram of Rocket Motor Plumbing System

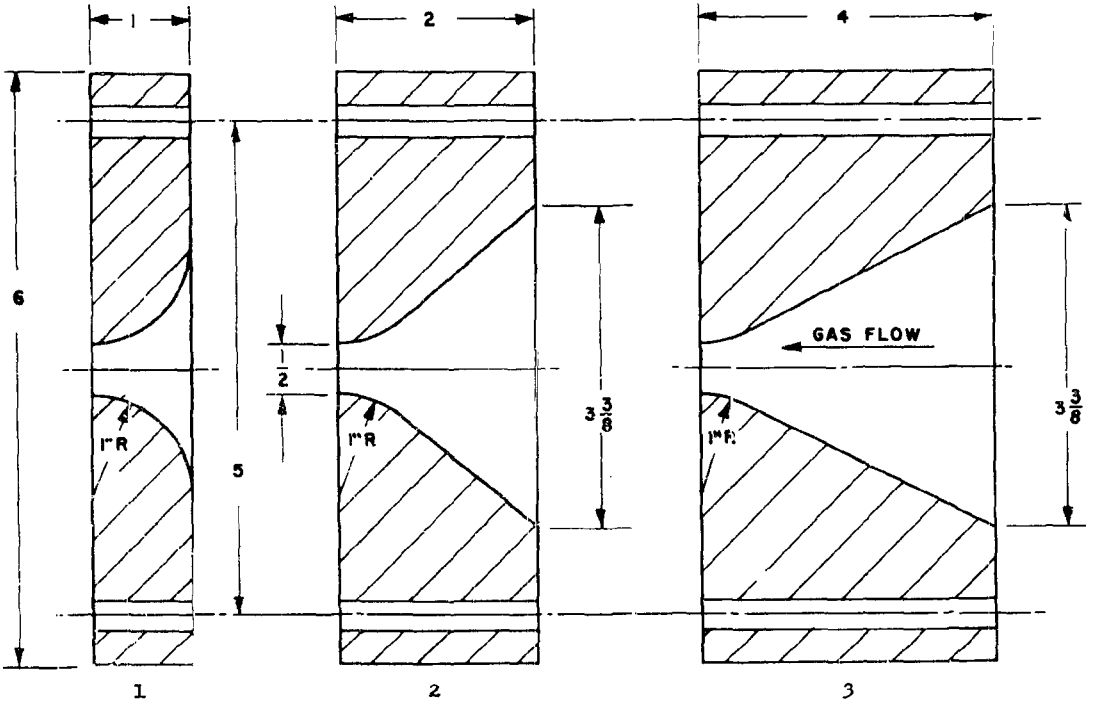

Fig. 4 Converging Nozzle Configurations.

ratio, and the steady state combustion pressure.

The locations of the pressure transducers were those described under the preceding sub-title.

EXPERIMENTAL RESULTS

1. Types of Combustion Pressure Oscillations

Figure 5 is an oscillograph record obtained from a gaseous bipropellant rocket motor burning propane and air, designated as PA, at a combustion pressure of 45 psia, with an equivalence ratio (E.R.) of 1.2, and a combustion chamber length of 22 5/8 inches. It is seen that the high frequency oscillations developed from what were initially low frequency oscillations; a similar phenomena has been reported by investigators using liquid bipropellant rocket motors (3).

Figure 6 is an oscillograph record obtained under identical operating conditions except that the length of the combustion chamber was 28 inches instead of 22 5/8 inches. It is seen from Fig. 6 that in this case high frequency combustion pressure oscillations developed following a period where the combustion pressure was uniform. There was no apparent initiating disturbance. It is apparent, however, that as the amplitude of the oscillations increase their wave changes. For convenience of description the term "sinusoidal oscillations" will be employed for describing those having a practically sinusoidal wave shape, and the term "shock type" for those having rapid rates of increase in pressure. It has been observed in the experiments conducted with gaseous bipropellant rocket motors at Purdue University that as the sinusoidal oscillations increase in amplitude they became transformed into the shock type of oscillations. Experimenters with liquid propellant rocket motors

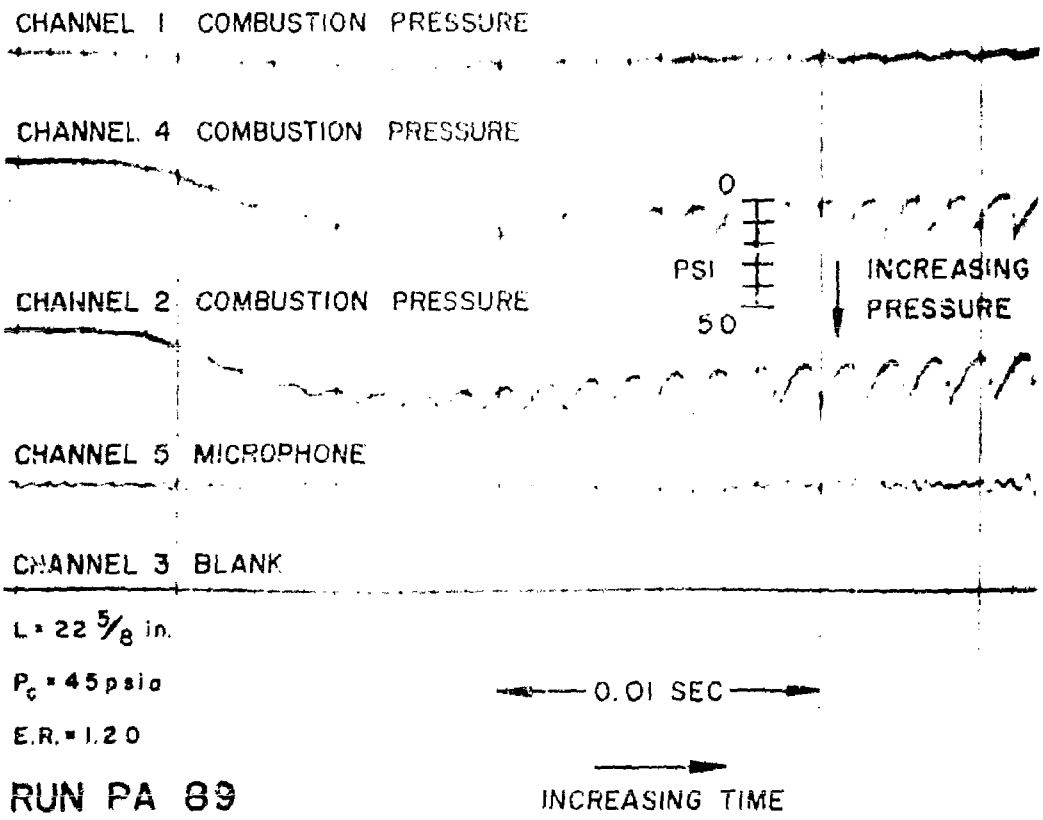

Fig. 5 Oscillograph Record Illustrating the Start of the Oscillations

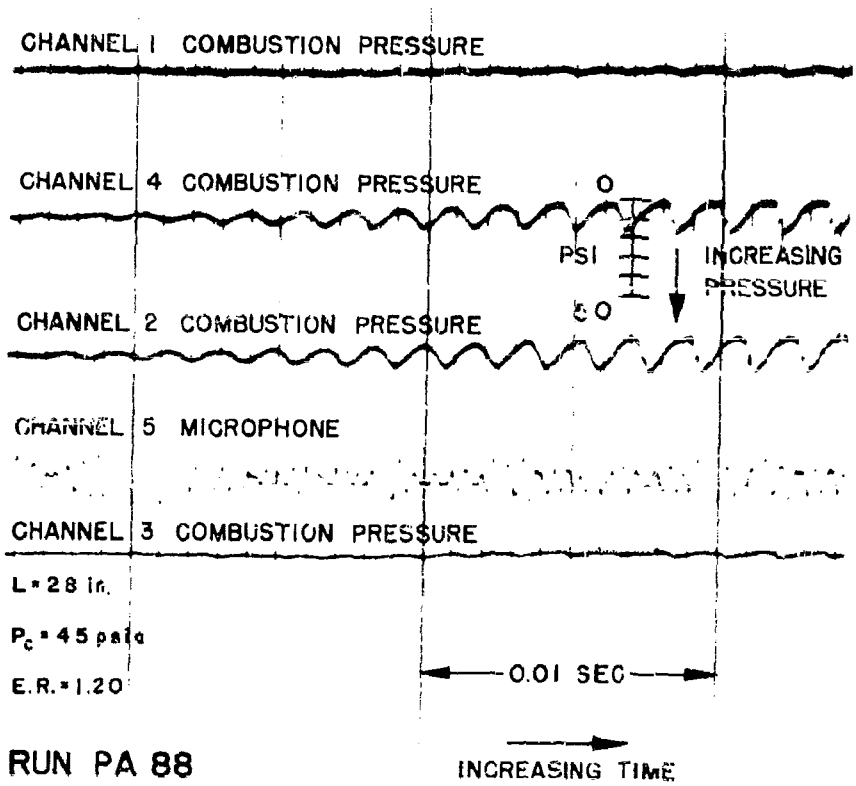

Fig. 6 Oscillograph Record Illustrating the Start of the Oscillations

have reported similar phenomena (4)(5)(6).

Figure 7 is a record obtained for the same conditions as for Fig. 6 except that the combustion chamber length was reduced to 22 5/8 inches. In this case the frequency of the combustion pressure oscillation is 5470 cps imposed upon an oscillation of 686 cps (see channel 2); the latter frequency corresponds to that for the fundamental longitudinal mode for the length of combustion chamber (22 5/8). On the other hand, the frequency of 5470 cps does not correspond to any harmonic of its longitudinal mode of oscillation.

Figure 8 illustrates the effect of reducing the length of the combustion chamber to 6 5/8 inches, all other variables remaining constant. Here again the oscillations have a frequency of 5470 cps, and as stated earlier they do not correspond to any longitudinal mode for the combustion chamber. It is concluded, therefore, that the 5470 cps oscillation is not a function of the length of the combustion chamber, and that the mode of the oscillation is one of the transverse types (radial or tangential).

2. Effect of Changing the Length of the Combustion Chamber

Figure 9 is an oscillograph record showing high frequency "shock type" oscillations of the longitudinal mode obtained from a propane-air rocket motor having a combustion chamber length of 28 inches; the equivalence ratio was 1.20.

Figure 10 presents typical oscillograms* for one cycle of the shock type of high frequency combustion pressure oscillations for the same

---

* An oscillogram is a photograph of the display on the face of the cathode ray tube of an oscilloscope.

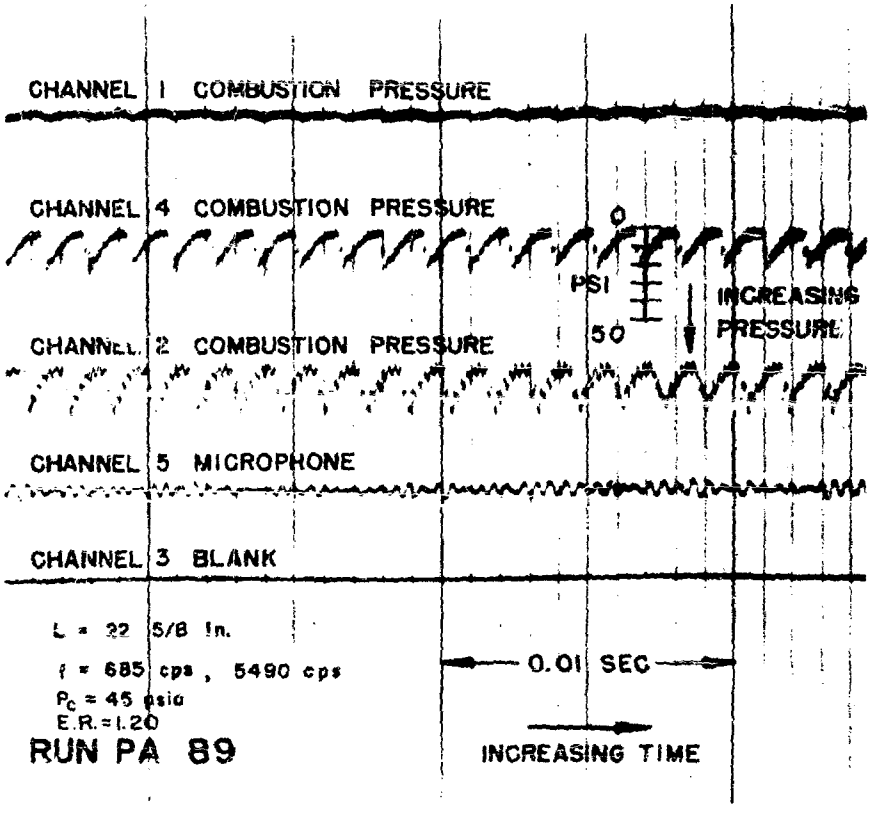

Fig. 7 Oscillograph Record Illustrating Transverse Mode of Oscillation

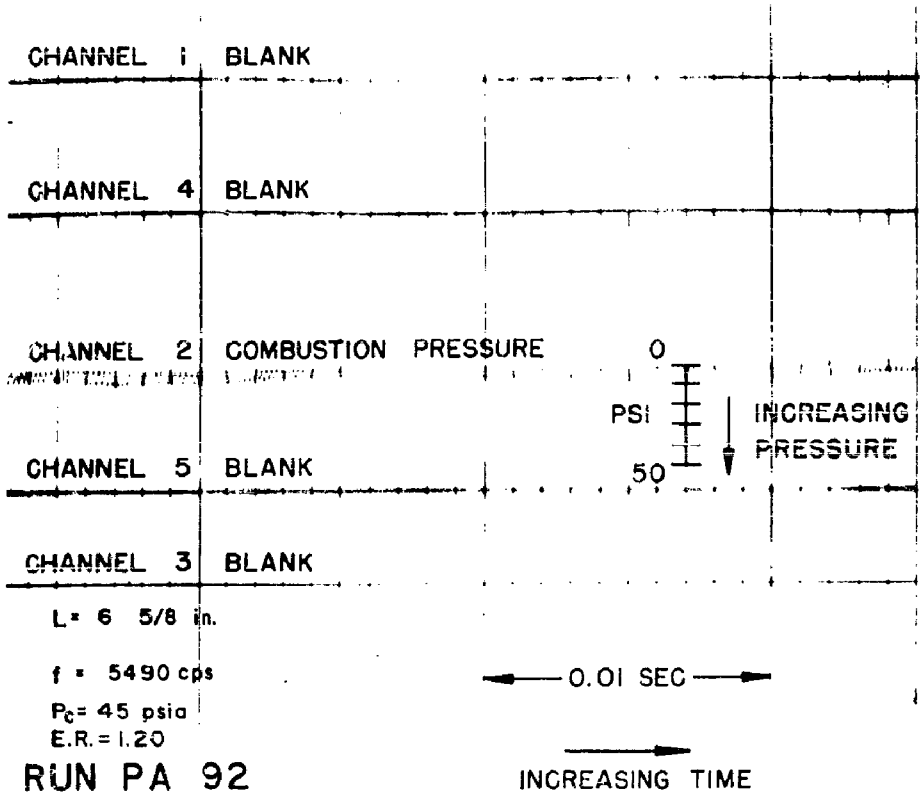

Fig. 8 Oscillograph Record Illustrating Transverse Mode of Oscillations

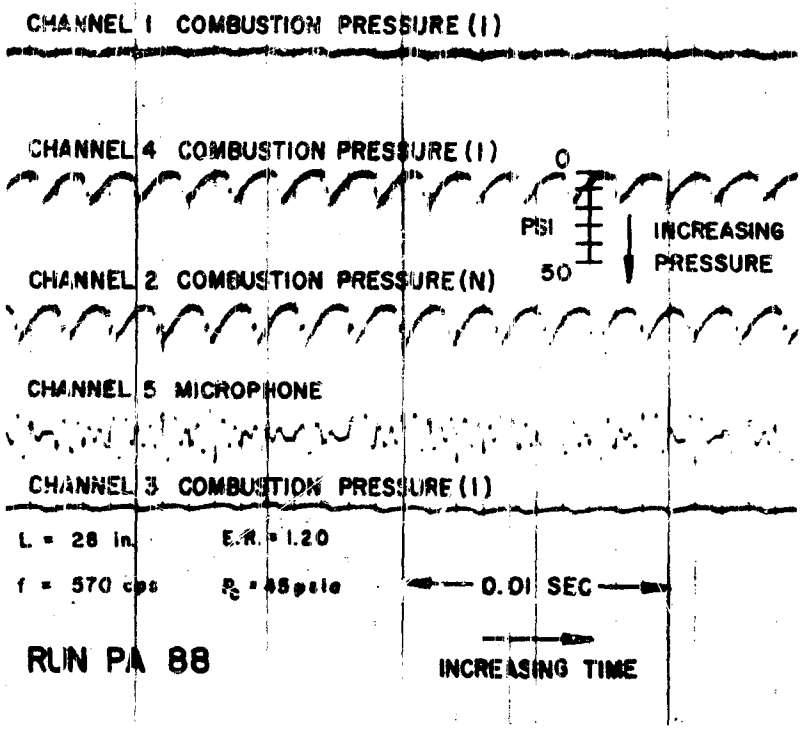

Fig. 9 Oscillograph Record Illustrating Oscillations of a Shock Type.

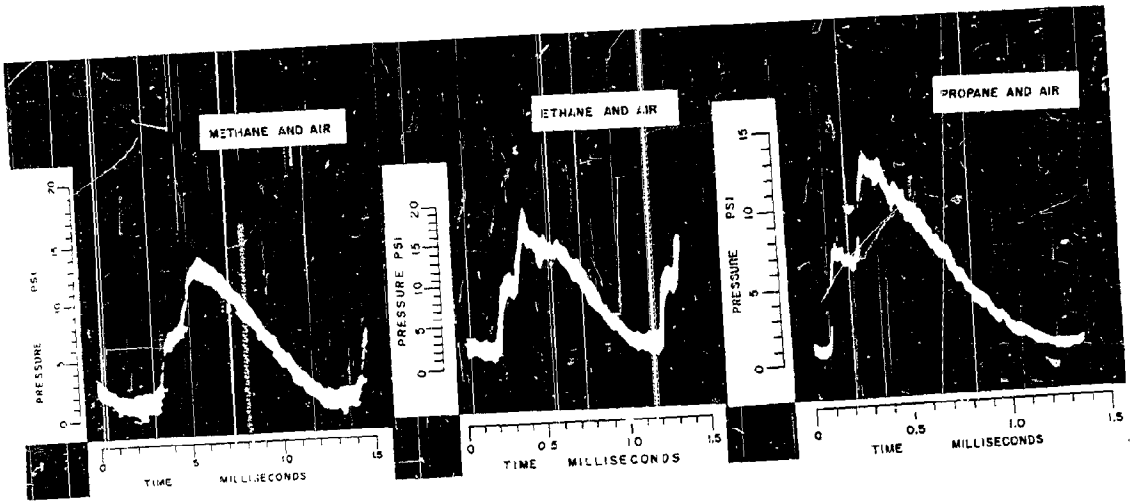

Fig. 10 One Cycle of the Shock Type Oscillation.

rocket motor burning (a) methane-air (b) ethane-air, and (c) propane-air. It is seen that in each case the pressure increase consisted of two rapid changes in pressure. The first occurred when a longitudinal pressure wave passed over the pressure sensing diaphragm of the Photocon transducer in moving from the nozzle toward the injector. The second pressure change is due to the same pressure wave being reflected from the face of the injector and again moving past the diaphragm of the Photocon transducer; from the injector towards the nozzle. From the oscillograms presented in Fig. 10 the rates of pressure rise obtained with the different gaseous propellants is readily determined. Thus for propane-air each pressure rise was approximately 7 psi and occurred in approximately 72 microseconds, giving a rate of pressure rise of approximately 97,200 psi per second, indicating that the pressure rise was due to a shock wave.

Figures 9, 11, 12, and 13 are oscillograph records from experiments with four rocket motors each having combustion chambers of the same diameter but different lengths. Figure 9 was obtained from a rocket motor having a combustion chamber length of 28 inches. Channel 2 in the figure presents the static pressure as measured by a Photocon transducer located in the wall of the combustion chamber 2 1/2 inches upstream from the entrance to the nozzle, and channel 4 is a record of the static pressure 2 1/2 inches downstream from the injector; the calibrations for channels 2 and 4 are also shown on the record. Channels 1 and 3 are static pressure records obtained from high pressure (2000 psi) transducers, and channel 5 is a record of the noise in the test cell as measured by a microphone. No information was taken from Channels 1, 3, and

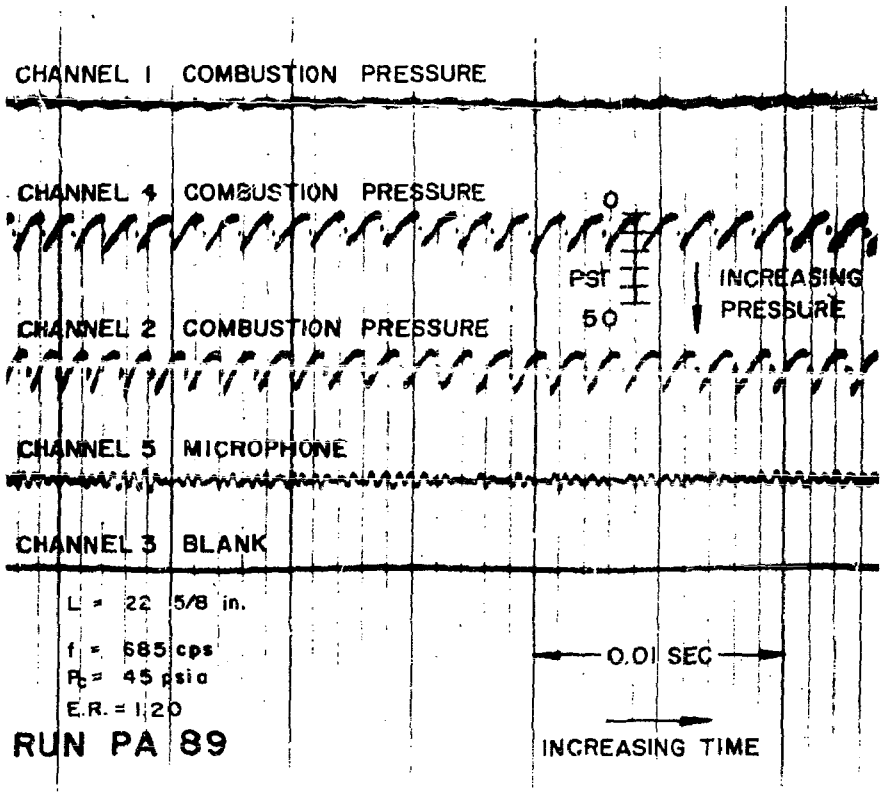

Fig. 11 Oscillograph Record

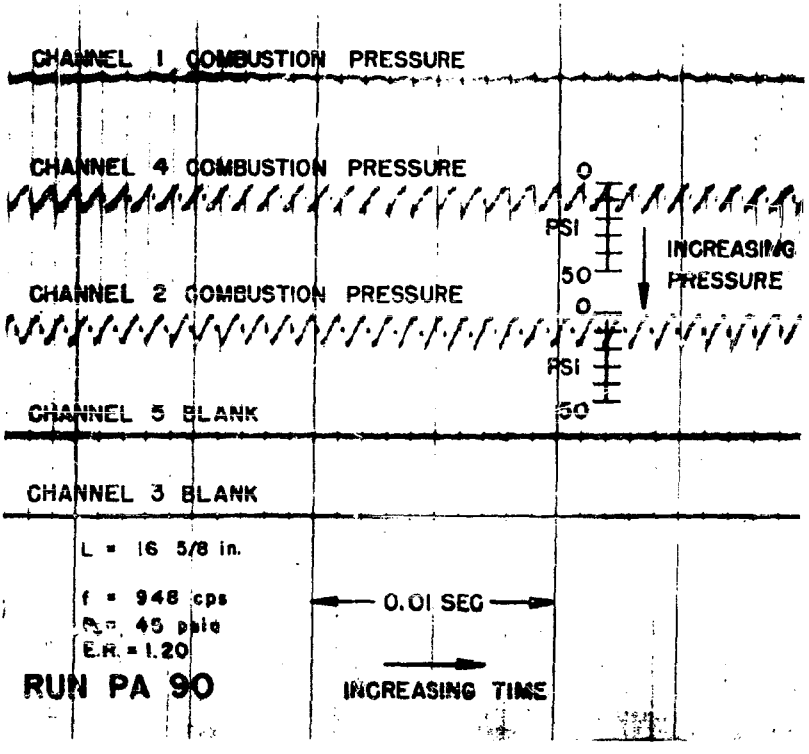

Fig. 12 Oscillograph Record

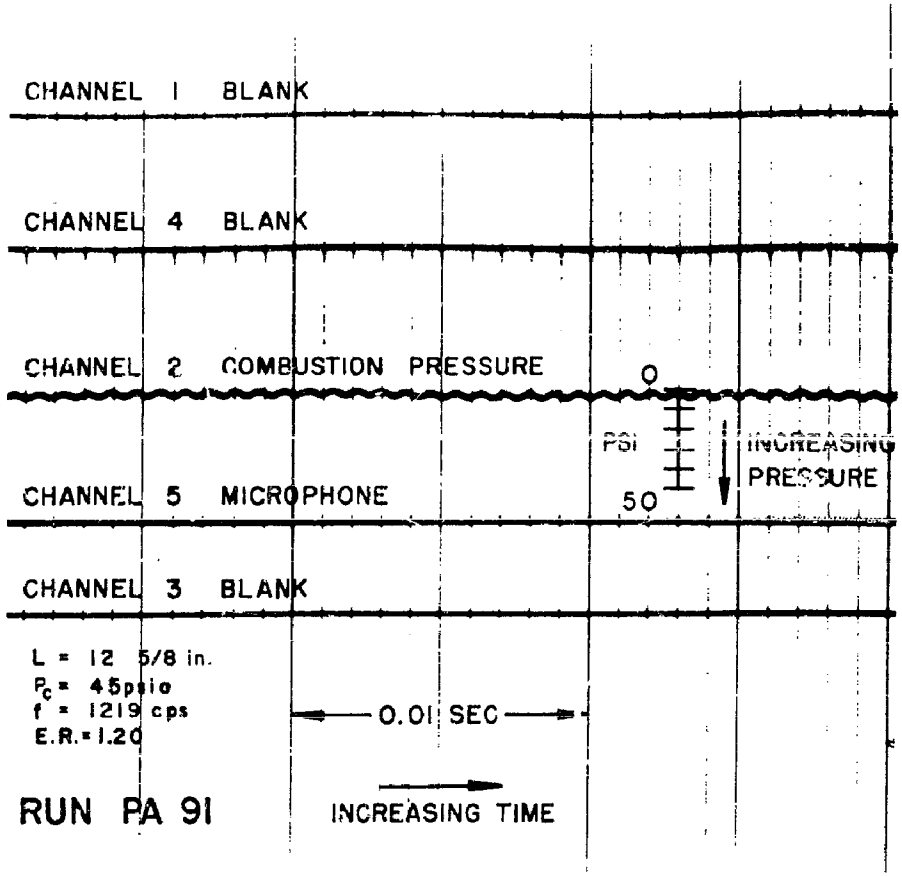

Fig. 13 Oscillograph Record

5. It is apparent from the records obtained from channels 2 and 4 that the combustion pressure oscillations were of the "shock" type, their frequency was 570 cycles per second, and their peak to peak amplitude was 22 psi.

Figure 11 illustrates the effect produced by reducing the length of the combustion chamber from 28 in. to 22 5/8 in. The 5 channels in Fig. 11 represent the same parameters as in Fig. 9; the pressure calibrations for channels 2 and 4 are shown on the record. It is seen, from channels 2 and 4, that the combustion pressure oscillations were of the "shock" type, their frequency was 685 cycles per second, and their peak to peak amplitude 22 psi.

Figure 12 is an oscillograph record obtained when the length of the combustion chamber was decreased to 16 5/8 in. Channel 2, in Fig. 16, presents the static pressure as measured by a Photocon transducer located in the wall of the combustion chamber 2 1/2 inches upstream from the entrance to the nozzle, and channel 4 presents the static pressure as measured by a Photocon transducer located in the wall of the combustion chamber 2 1/2 inches downstream from the injector; the pressure calibrations for channels 2 and 4 are shown on the record. Channel 1 is a static pressure record obtained from a high pressure (2000 psi) transducer, and channels 3 and 5 had no input applied to them. The records obtained from channels 2 and 4 indicate that the combustion pressure oscillations are of the "shock" type, their frequency was 948 cycles per second, and their peak to peak amplitude 17 psi.

Figure 13 is the record obtained from a rocket motor having a combustion chamber length of 12 5/8 inches. Channel 2, in Fig. 13, presents

the static pressure as measured by a calibrated Photocon transducer located in the wall of the combustion chamber 2 1/2 inches upstream from the entrance to the nozzle. It is seen, from channel 2, that the combustion pressure oscillations were of the "sinusoidal" type, their frequency was 1219 cycles per second, and their peak to peak amplitude 3.5 psi.

Figure 14 presents the frequency of the combustion pressure oscillations, as obtained from the oscillograph records, as a function of the length of combustion chamber for five different values of combustion chamber length for the case where the propellants were propane-air burned under the conditions indicated in the figure. Experiments conducted with the propellant combinations methane-air, ethane-air, and ethylene-air yielded similar relationships between the frequency of the oscillations and the length of the combustion chamber.

Figure 15 presents the amplitude of the combustion pressure oscillations as a function of the length of the combustion chamber for the propellant combinations of methane-air, ethane-air, and ethylene-air. In all of the experiments the pressure drops in the air and fuel lines, and the steady-state combustion pressure were held constant. The variables were the combustion chamber length and the equivalence ratio. The curves in Fig. 15 were obtained by plotting the largest amplitude of the pressure oscillation for a given length of combustion chamber. The frequency and magnitude of the oscillations were obtained from oscillograph records such as those presented for propane and air.

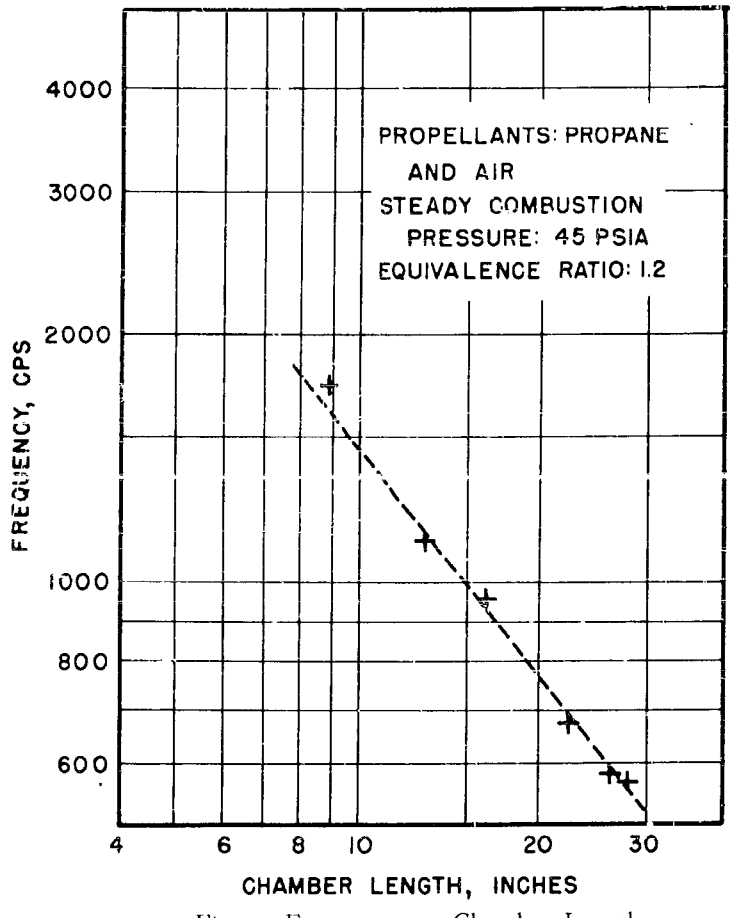

Fig. 14 Frequency vs. Chamber Length

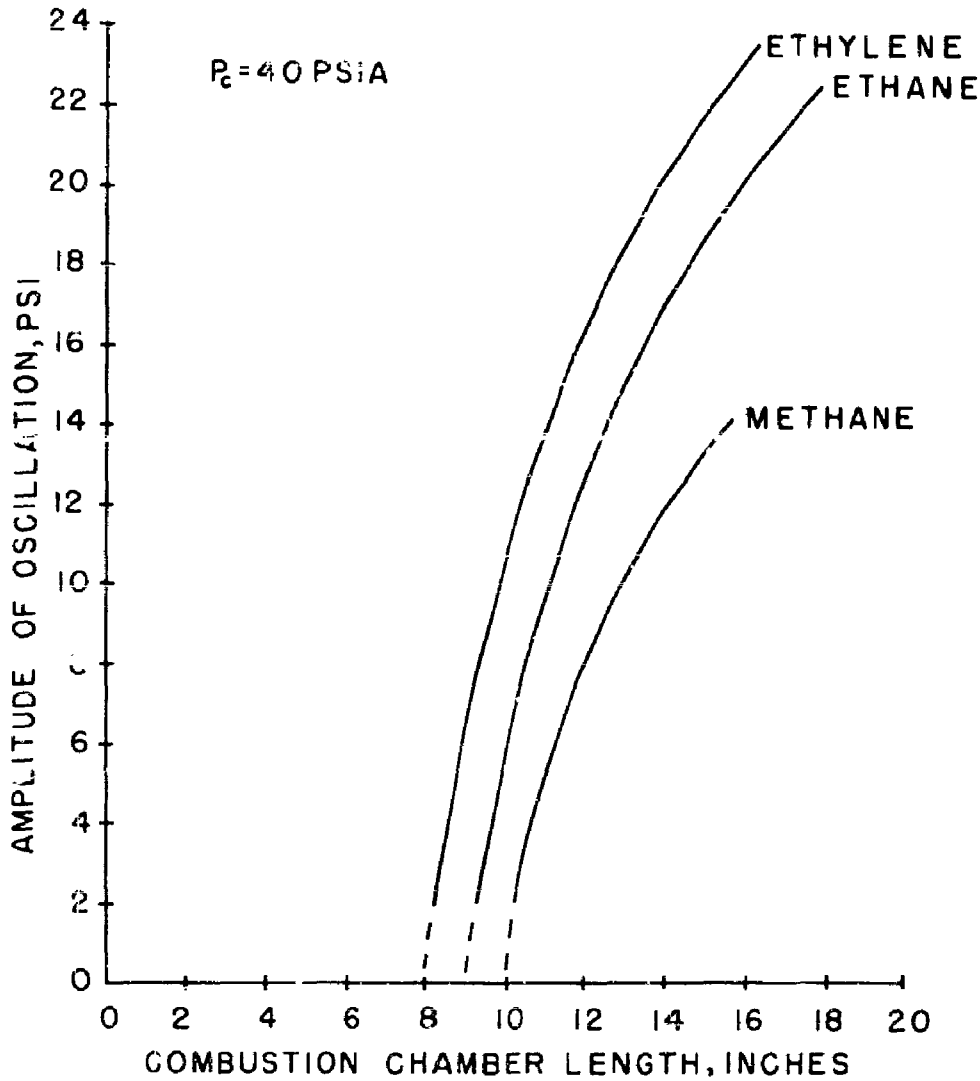

Fig. 15 Length vs. Amplitude of Oscillations

3. Effect of Changing the Equivalence Ratio

These experiments were conducted for the purpose of determining the influence of the equivalence ratio upon the susceptibility of a rocket motor to combustion pressure oscillations. The experiments were conducted with the following propellant combinations; methane-air, ethane-air, and ethylene-air. In all of the experiments the length of the combustion chamber was 16 1/4 inches, and the same exhaust nozzle (No. 1, Fig. 3) was employed. The steady-state combustion pressure was varied from 20 to 210 psia and the equivalence ratios from approximately 0.4 to 1.4.

Figure 16 is a typical oscillograph record from a run using ethane and air as propellants wherein the steady-state combustion pressure was 88 psia and the equivalence ratio was 0.990, and Fig. 17 is one for the same propellants for a steady-state combustion pressure of 113 psia and an equivalence ratio of 0.991. Four Photocon pressure transducers were used in the experiments. Channels 1, 3, and 4 of the oscillograph records shown in Figs. 16 and 17 present the static pressure as measured by a Photocon pressure transducer located 2 1/2 inches downstream from the injector face. Channel 2 presents the static pressure as measured by a Photocon pressure transducer located 2 1/2 inches upstream from the nozzle face.

Figure 18 is an oscillograph record obtained using methane and air as the propellants and illustrates the transverse oscillations encountered when the steady-state combustion pressure is increased over 150 psia. The steady-state combustion pressure was 210 psia and the equivalence ratio was 0.670. Channel 2 presents the static pressure measured by a

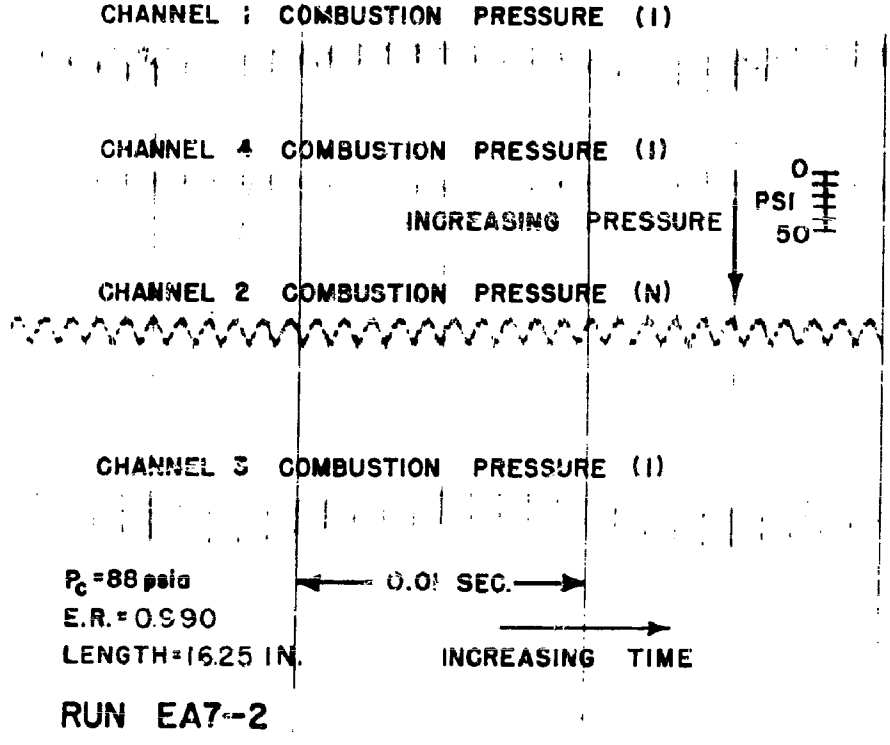

Fig. 16 Oscillograph Record for Ethane and Air.

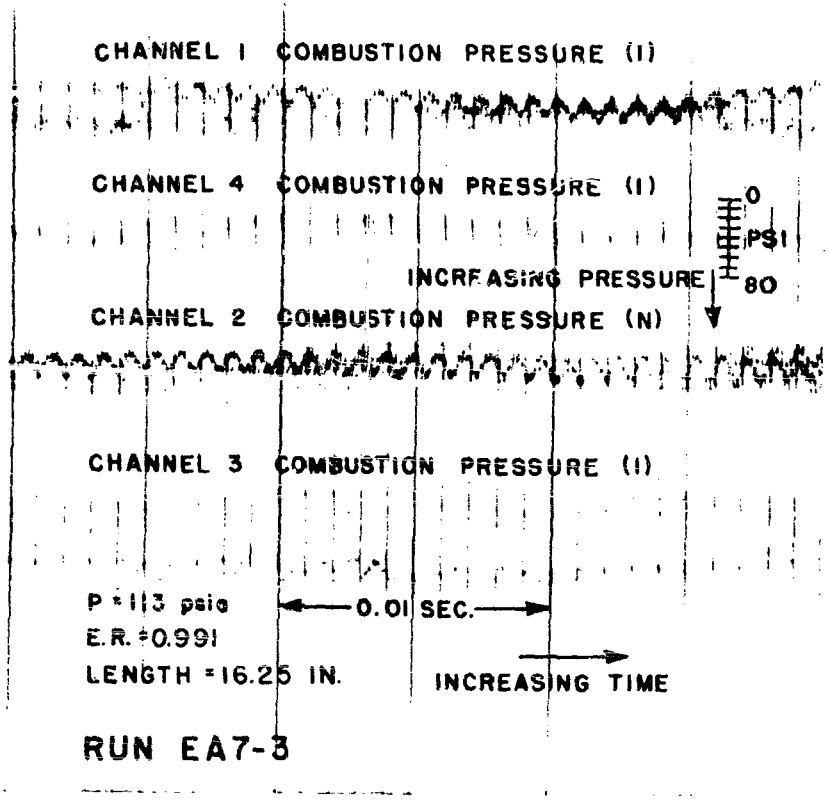

Fig. 17 Oscillograph Record for Ethane and Air.

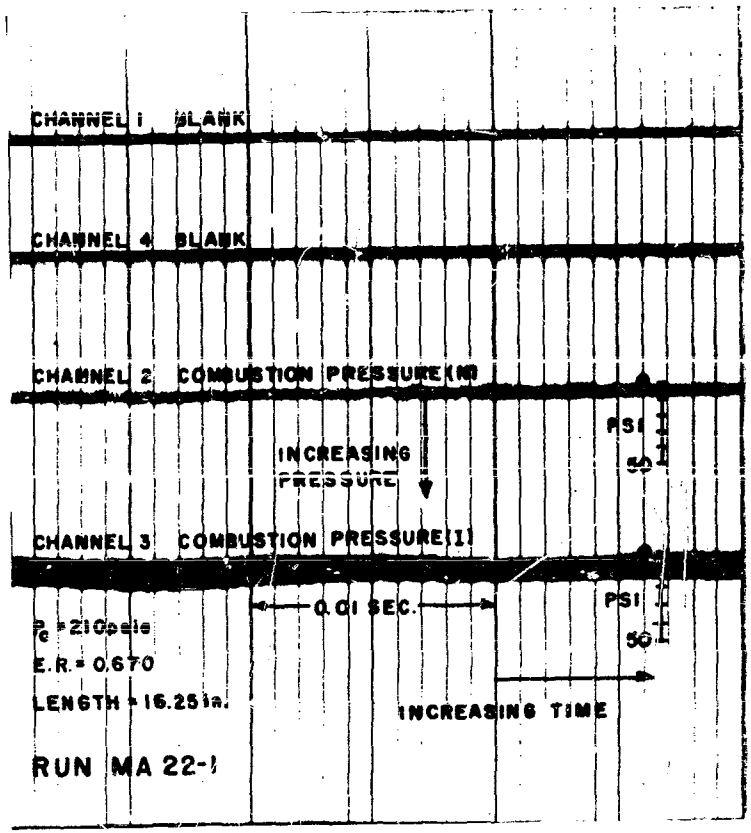

Fig. 18 Oscillograph Record for Methane and Air

Photocon pressure transducer located 2 1/2 inches upstream from the nozzle face and channel 3 presents the static pressure as measured by a Photocon pressure transducer located 2 1/2 inches downstream from the injector face.

Figures 16, 17, and 18 illustrate the effect produced by increasing the combustion pressure from 88 to 210 psia. It can be seen that as the steady-state combustion pressure is increased, the oscillations transform from a longitudinal to a transverse mode.

Figure 19 presents the equivalence ratio as a function of the mean combustion pressure for the above series of experiments. The curves represent the limits of regions wherein longitudinal combustion pressure oscillations occurred for the different propellant combinations.

4. Effect of Nozzle Configuration

Figures 20, 21, and 22 present oscillograph records illustrating the effect of nozzle configuration upon the wave form of the combustion pressure oscillations, for a rocket motor burning methane and air. In these experiments the steady-state combustion pressure, the combustion chamber length, and the equivalence ratio were held constant and different nozzles having the same throat diameters were employed. The configurations of the nozzles are shown in Fig. 3.

Figure 20 is an oscillograph record illustrating combustion pressure oscillations which occurred when Nozzle No. 1 (see Fig. 3) was employed.

Figure 21 was obtained with Nozzle No. 2 (see Fig. 3) and Fig. 22 with Nozzle No. 3.

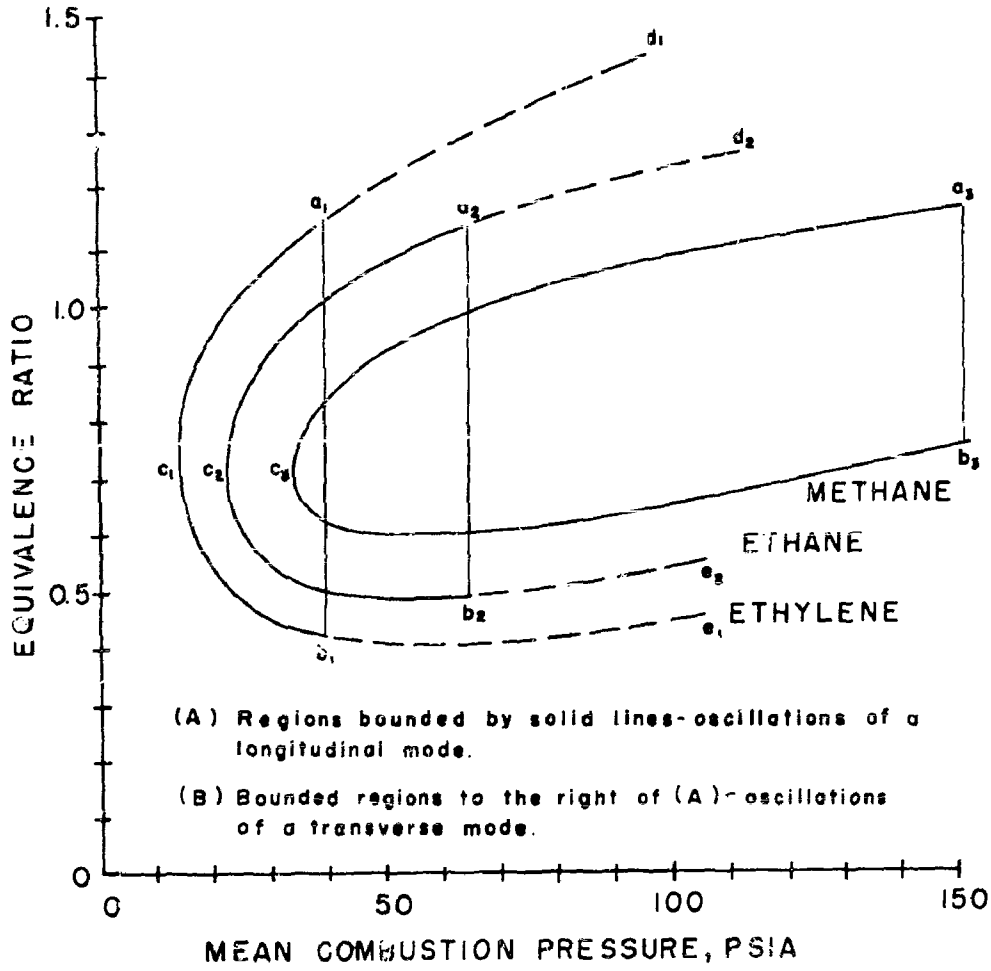

Fig. 19 Stability Regions

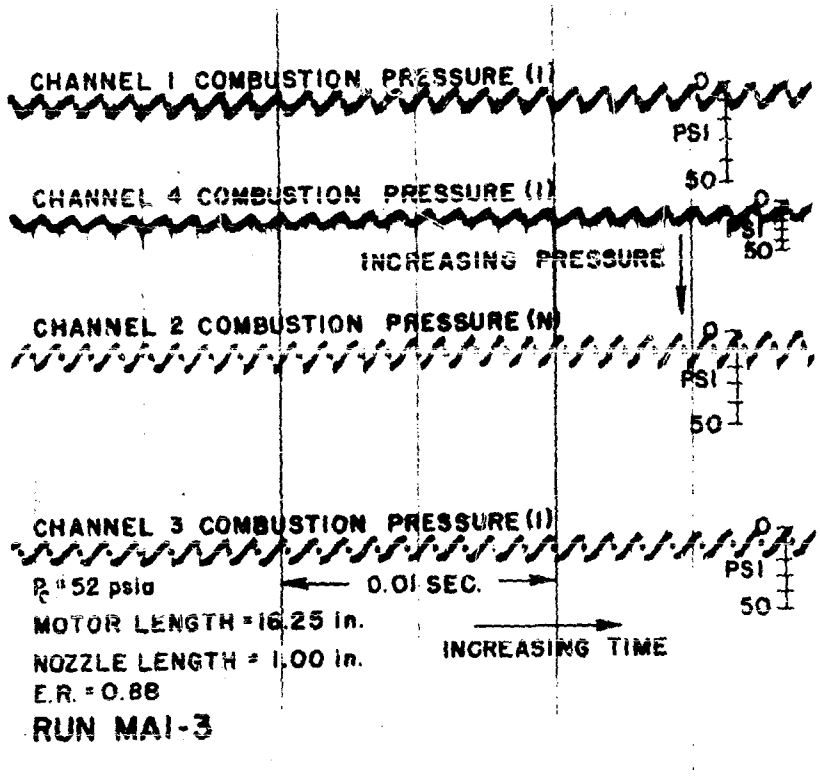

Fig. 20 Oscillograph Record for Methane and Air.

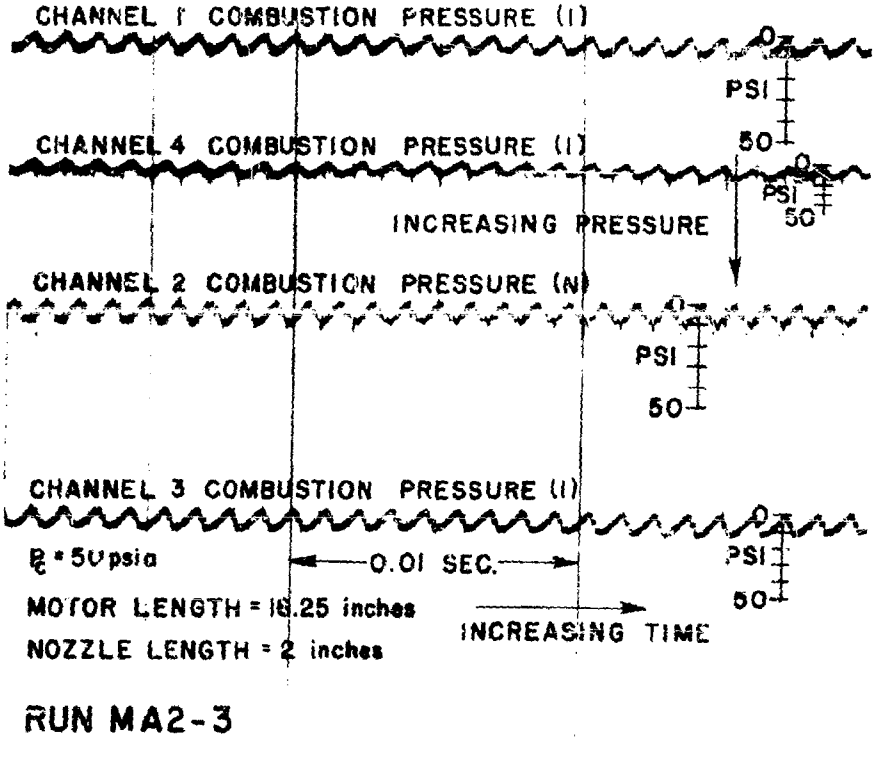

Fig. 21 Oscillograph Record for Methane and Air.

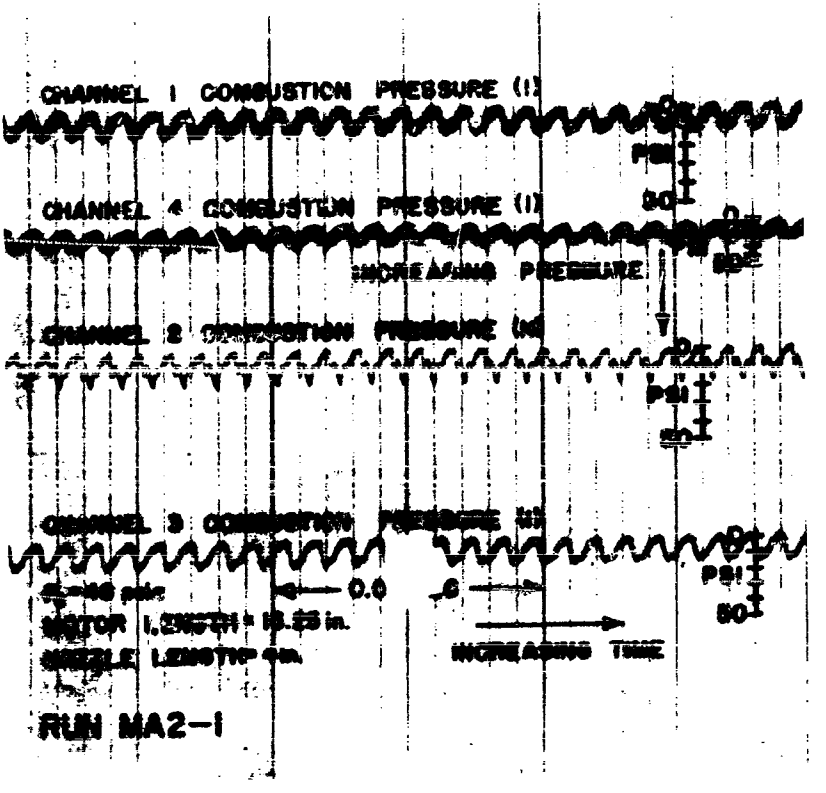

Fig. 22 Oscillograph Record for Methane and Air.

In all of the experiments channels 1, 3, and 4 present the combustion pressure measured by a Photocon pressure transducer located 2 1/2 inches downstream from the face of the injector, and channel 2 that measured 2 1/2 inches upstream from the entrance section of the exhaust nozzle.

By comparing the records obtained from channel 2 in each of the afore-mentioned oscillographs it is seen that changing the nozzle configuration alters the wave form of the longitudinal combustion pressure oscillations from the "shock" type. It appears that by properly shaping the entrance section of the nozzle the amplitude of the oscillations may be reduced to an insignificant value.

DISCUSSION OF RESULTS

1. Effect of Length of Combustion Chamber

A. Longitudinal Mode

Figures 14 and 15 illustrate the effect of changing the length of the combustion chamber upon the frequency and amplitude of the combustion pressure oscillations of the longitudinal mode. The curves show that the length of the combustion chamber has a decisive influence upon the frequency, amplitude, and type of combustion pressure oscillations of the longitudinal mode. The following mechanism is postulated for explaining the influence of the length of the combustion chamber upon the characteristics of the combustion pressure oscillations of the longitudinal mode.

Consider a small pressure disturbance traveling longitudinally downstream from the injector toward the nozzle. During the time that the pressure disturbance is moving in the downstream direction, the combustion process in the neighborhood of the injector proceeds at a normal rate. After the pressure disturbance is reflected upstream from the entrance section of the nozzle it traverses the recently ignited and unburned propellants as it moves toward the face of the injector. The pressure wave compresses the unburned and burning mixture traversed by it thereby increasing the combustion temperature and pressure and consequently the heat-release rate. Because of the increased rate of heat-

release the pressure disturbance becomes amplified because of the increased rate of production of hot combustion gases; the latter rate exceeds that corresponding to the steady-state combustion pressure. The amplified pressure disturbance is reflected from the injector face and again traverses the unburned mixture augmenting the burning rate and consequently further amplifying the pressure disturbance.

In a rocket motor having a short tubular combustion chamber, the time for a pressure disturbance to travel twice the length of the combustion chamber is short. Consequently, only a small amount of combustible mixture is injected into the combustion chamber during the time required for two successive reflections of a pressure wave from the face of the injector. The smaller the quantities of burned and burning propellants traversed by a pressure disturbance the smaller is the energy release, and consequently the amplitude of the combustion pressure oscillations. It is conceivable that if the combustion chamber is short enough the amplitude of the combustion pressure oscillations of the longitudinal mode may become insignificant.

Increasing the length of the combustion chamber increases the time required for a pressure disturbance to traverse twice the length of the combustion chamber. Simultaneously, the quantities of unburned and burning propellants present in the combustion chamber between successive reflections of the pressure wave are increased. One may, therefore, expect an increased amplification of combustion pressure because of the larger amount of thermochemical energy released by the pressure wave compressing the larger amounts of unburned and burning propellants. It is conceivable, however, that if the combustion chamber were made sufficiently

long the pressure disturbance will be considerably attenuated before it can traverse twice the length of the combustion chamber. Thus the returning pressure wave could be too weak for raising the temperature and pressure of the unburned and burning mixture significantly, and, therefore, there would be no amplification of the pressure disturbance.

The experimental results presented in Figs. 9, 11, 12, and 13 appear to confirm the mechanism postulated in the foregoing. No data were obtained, however, for combustion chamber lengths exceeding 28 inches. Comparison of Figs. 9 and 11, for the longer chambers (28 and 22 5/8 inches respectively) with Figs. 12 and 13, shows that the amplitudes of the oscillations for the longer chambers were larger than for the shorter chambers. Furthermore, in the experiments with a combustion chamber 6 5/8 inches long, no high frequency combustion pressure oscillations of the longitudinal mode could be initiated.

B. Transverse Mode

Figure 7 shows the presence of an oscillation having a frequency of 5470 cps superimposed on the longitudinal mode. Regardless of the length of the combustion chamber, the presence of that frequency was noted in all of the propane-air experiments which exhibited the transverse superimposed upon the longitudinal mode.

Moreover, the frequency of 5470 cps does not correlate with the fundamental frequency or any harmonic of a longitudinal acoustic mode. It is concluded, therefore, that the 5470 cps frequency is some form of transverse mode of combustion pressure oscillation, that is, radial, sloshing, or spinning (see Fig. 1).

No detailed information could be obtained regarding the 5470 cps oscillation because the Photocon pressure transducers were located so that only the longitudinal mode could be identified. It is planned to make a detailed study of the transverse modes of oscillation by employing rocket motors having larger diameter combustion chambers, so that the identification of the various transverse modes will be simpler.

C. Comparison of the Experimental Results with a Mathematical Analysis

Figure 23 shows the frequency of a longitudinal mode in cps as a function of the combustion chamber length in inches. The curve labeled "Theoretical" was computed from the following equation derived by Tischler et al (7).

$$f = \frac{0.36\ nC^*}{L}$$

where

f is the frequency of the longitudinal oscillation in cps,

n is a harmonic factor,

C* is the characteristic velocity in ft/sec.

L is the length of combustion chamber in ft.

The curve marked "Experimental" is the same as that presented in Fig. 14 for the propane-air propellants.

It is seen that the experimental values for the frequency of the oscillations compare favorably with the calculated values, even though the assumptions employed in deriving the equation limit its application to systems having no energy addition within a cycle, a constant velocity for the speed of sound, and no steady-state velocity through the system.

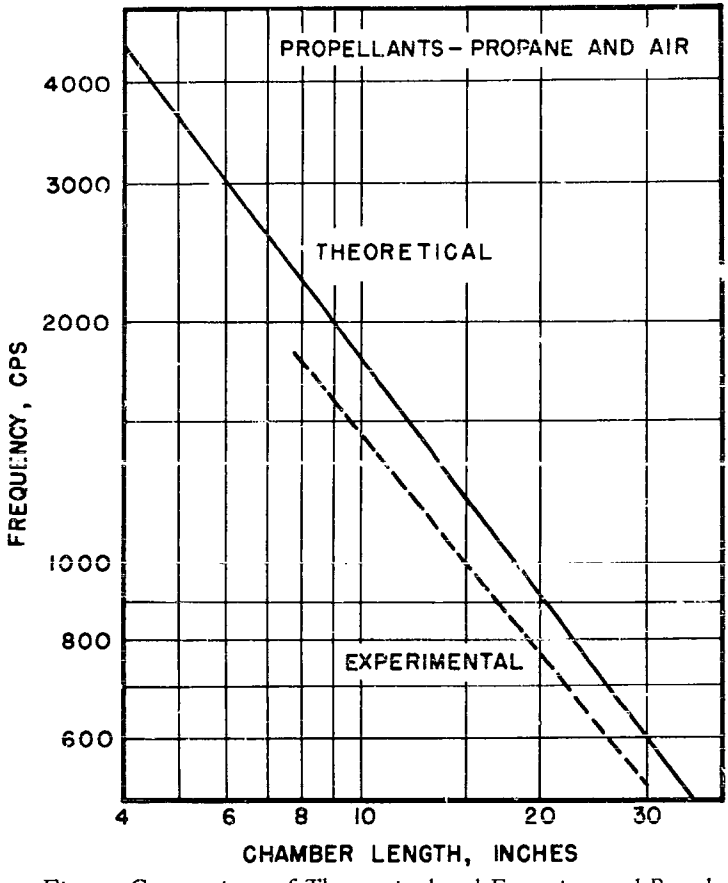

Fig.23 Comparison of Theoretical and Experimental Results for Frequency vs. Chamber Length

Actually, apart from aiding in identifying the mode of the oscillation, little is gained by comparing the experimental and calculated values of frequency.

Other theories are based upon the concept of a time lag (8). A part of the time lag includes vaporization and mixing of the propellants but these processes are absent in the rocket motor employed in the experimental work reported herein; the propellants were premixed gases prior to their injection into the combustion chamber. No comparison was, therefore, made with the theoretical results of the afore-mentioned type of theory.

2. Steady-State Combustion Pressure-Equivalence Ratio Experiments

Figure 19 presents the equivalence ratio as a function of the mean combustion pressure for the methane-air, ethane-air, and ethylene-air propellants. The curves shown in the figure delineate the regions of stable combustion, combustion pressure oscillations of a longitudinal mode, and oscillations of a transverse mode. To illustrate, for the ethylene-air propellants no oscillations were observed in the region to the left of the curve $a_1b_1c_1$. In the region enclosed by $a_1b_1c_1$ the oscillations were of a longitudinal mode, but in the region enclosed by $d_1a_1b_1e_1$ they were of a transverse mode. For methane and air the region wherein the combustion was oscillatory covered the smallest range of equivalence ratios for the propellant combinations investigated. On the other hand, combustion pressure oscillations were encountered with the ethylene-air propellants over the widest range of equivalence ratios.

It is possible to relate the stability regions to the heat-release rates for the propellant combinations. The rate of heat-release for a

propellant combination (see Appendix C) depends upon (a) the combustion pressure, and (b) the equivalence ratio. Since the length of combustion chamber exceeds its diameter, it takes longer for a longitudinal combustion pressure wave to traverse the combustion zone than it does for a transverse wave. Consequently, a lower heat-release rate is required for sustaining a longitudinal than a transverse oscillation. Increasing the steady-state combustion pressure, however, may increase the heat-release rate sufficiently so that only the transverse oscillations can be sustained. It appears, therefore, that beyond a certain critical steady-state combustion pressure (150 psia for methane and air) only oscillations of a transverse mode will occur, and below that combustion pressure the longitudinal mode appears. The ethylene-air mixture has higher heat-release rates at a given initial combustion pressure than the other propellants. Consequently, for the reasons given above the transition from the longitudinal to the transverse oscillations occurs at lower steady-state combustion pressures for ethylene-air than for methane-air.

Figure 24 illustrates qualitatively the effect of the equivalence ratio upon the heat-release rates of mixtures of methane and air, ethane and air, and ethylene and air (8)(9)(10). It is seen from Fig. 24, that for a given heat-release rate the range of equivalence ratio is larger for ethylene than for methane and ethane. Thus, the range of equivalence ratios in which combustion pressure oscillations could occur for ethylene would be greater than those for methane and ethane.

When the steady-state combustion pressure for methane and air exceeds approximately 150 psia the range of equivalence ratios giving combustion

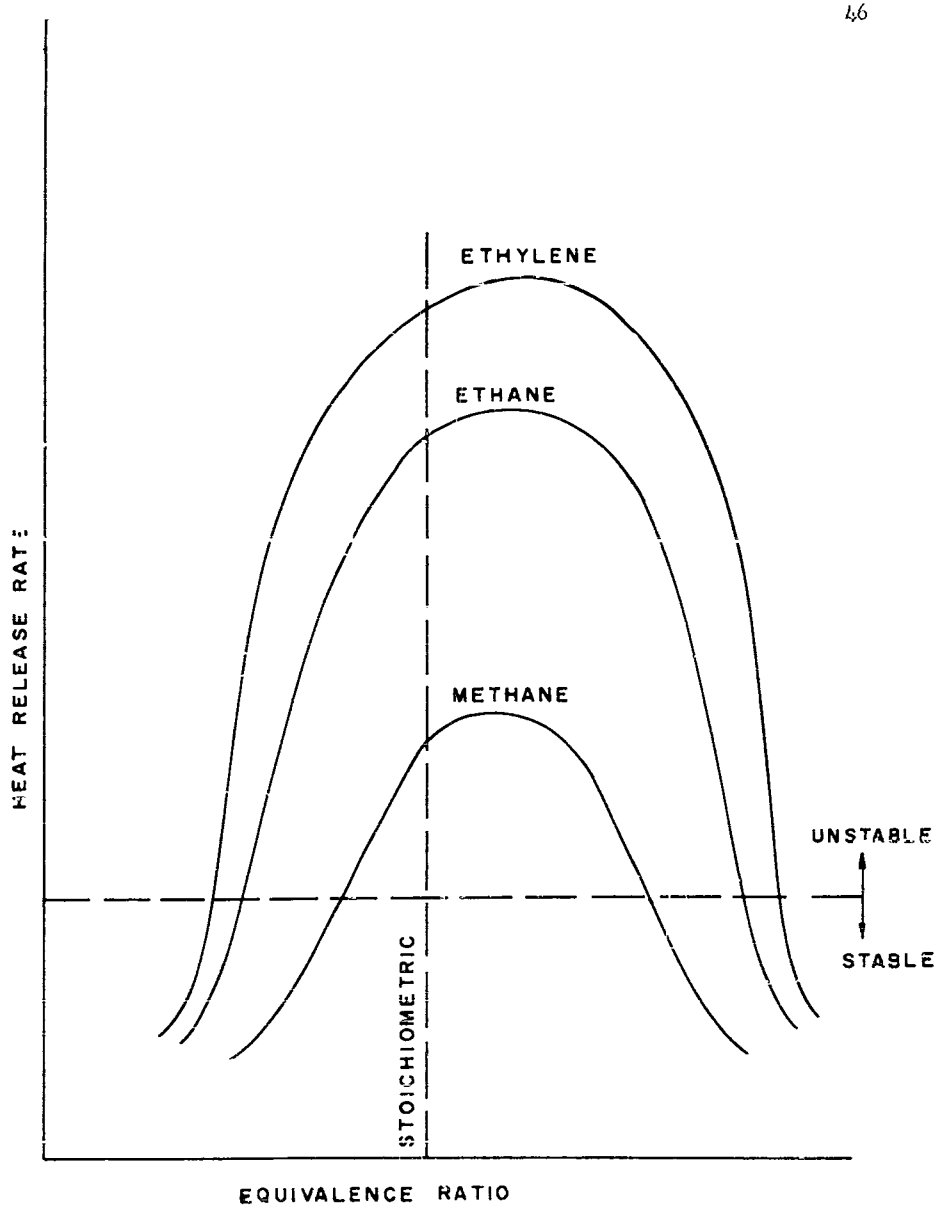

Fig. 24 Heat Release Rate vs. Equivalence Ratio

pressure oscillations of a longitudinal mode is quite narrow. At combustion pressures above 150 psia the amplitudes of the longitudinal combustion pressure oscillations become very small (less than 5 psi), but large amplitude transverse combustion pressure oscillations may occur (see Fig. 18).

For the ethane-air propellants the combustion pressure oscillations transform from a longitudinal to a transverse mode at a lower steady-state combustion pressure than for the methane-air propellants. The ethylene-air combination has the highest heat-release rate of the propellants investigated, and with those propellants combustion oscillations of a longitudinal mode transformed into oscillations of a transverse mode at combustion pressures as low as 40 psia.

For all of the propellants investigated no oscillations were observed below some value for the steady-state combustion pressure. At those low pressures, the propellant flow rates are small and the amount of energy supplied per unit time to the combustion zone was insufficient for driving a combustion pressure oscillation.

3. Effect of Nozzle Configuration

A comparison of Figs. 20 and 21 indicates that a slight configuration change in the converging portion of the nozzle has no appreciable influence upon the wave shape of the combustion pressure oscillations.

Figure 22 illustrates that the wave shape of the oscillation shown in channel 2 (the Photocon transducer located 2 1/2 inches upstream of the nozzle entrance) differs markedly from that of the shock type. The difference may be attributed to the face that the entrance section of the

nozzle no longer affords a surface from which pressure waves can be reflected in the longitudinal direction with full intensity but causes the reflected pressure waves to interfere with each other.

CONCLUSIONS AND RECOMMENDATIONS

From the experiments performed thus far under Phases I and II of the program, it is apparent that little is known of the mechanism whereby high frequency combustion pressure oscillations are initiated, amplified and attenuated.

The experiments discussed herein were conducted with premixed gases as the propellants. The time lags for vaporizing and mixing the propellants, present in the case of liquid propellants, were absent (11). Nevertheless, high frequency combustion pressure oscillations were obtained. It appears probable that the time lag required for vaporizing and mixing liquid propellants may not be a predominating factor in the initiation of high frequency combustion pressure oscillations. More investigation is needed to establish that point.

The experiments indicate that the rate of heat-release of a propellant combination is an important factor in initiating high frequency combustion pressure oscillations; the normal burning velocity was the property employed for comparing the heat-release rates of premixed gases.

The experiments demonstrate that the geometry of the combustion chamber exercises a decisive influence in initiating and sustaining the high frequency combustion pressure oscillations. Furthermore, the configuration of the exhaust nozzles affects the wave form of the high frequency combustion pressure oscillations.

Although transverse combustion pressure oscillations were observed in the experiments, insufficient studies of that phenomena were made for deducing general conclusions. Research has been planned, employing larger diameter motors, for making a more complete study of the transverse modes of oscillation.

It is planned to expand the experimental program concerned with the influence of heat-release rates upon the high frequency combustion pressure oscillations. It is also planned to study the effect of changing the location of the propellant injection system and also the influence of fuel additives upon the high frequency combustion pressure oscillations.

A P P E N D I C E S

APPENDIX A

NOTATION

A - Arrhenius constant

C_f - local concentration of fuel

C_o - local concentration of oxidizer

C* - characteristic velocity

e - 2.71828

E - activation energy

EA - ethane-air

EyA - ethylene-air

E.R. - equivalence ratio

F - function of the transport properties of the system

f - frequency

g - acceleration of gravity

K - a constant

L - length of the combustion chamber

MA - methane-air

P_c - combustion pressure

p - local pressure

Q - heat release rate per unit volume

R - gas constant

S - experimental flame speed

T - local temperature

T_f - adiabatic flame temperature

W - reaction rate

ϵ - portion of fuel remaining unburnt

APPENDIX B

DESCRIPTION OF APPARATUS

INSTRUMENTATION AND MEASUREMENTS

1. General Description. Figure 25 illustrates schematically a plan view of the test cell, propellant supply tanks, and control room. All of the rocket motor experiments described herein were conducted in the above test cell. The control panel for remote operation of the rocket motor and also the requisite instruments for recording the data were located in the control room.

2. Control Room. The control room contained the "firing control console," the indicating and the recording pressure gages for steady-state readings, the high frequency pressure measuring instrumentation, the temperature indicators, and the instruments giving the steady-state flow rates of air and fuel. Figure 26 illustrates the arrangement of the apparatus. All of the operations of the rocket motor were controlled from the "firing control console" which contained all of the requisite control switches.

3. Test Cell. Figure 27 is a photograph of a rocket motor mounted on the thrust stand in the test cell. The latter housed the rocket motor, the thrust stand, and the fuel and air feed lines and their associated apparatus.

4(a). Air Supply System. High pressure air at approximately 1500 psig was supplied to the pressure reducing system illustrated in Fig. 3. By

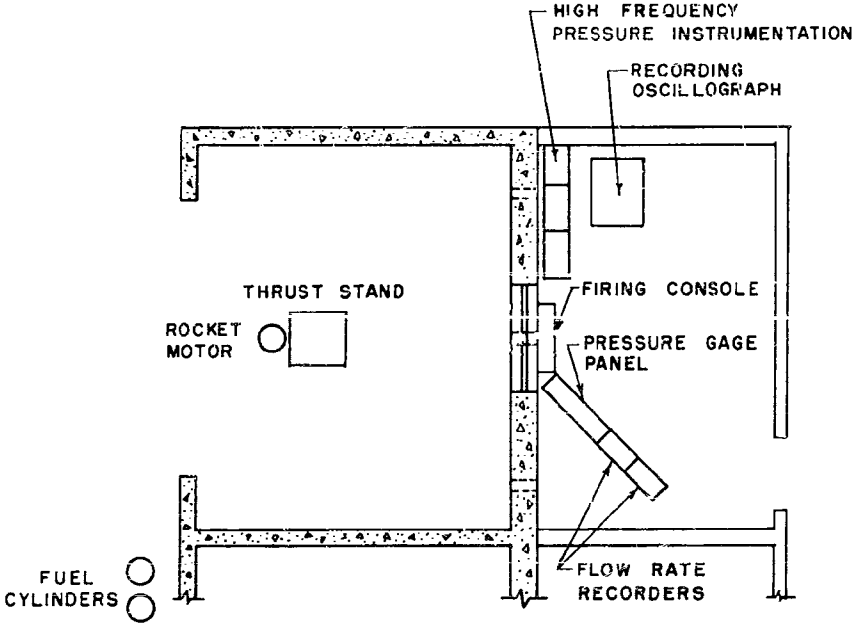

Fig. 25 Plan View of Test Cell

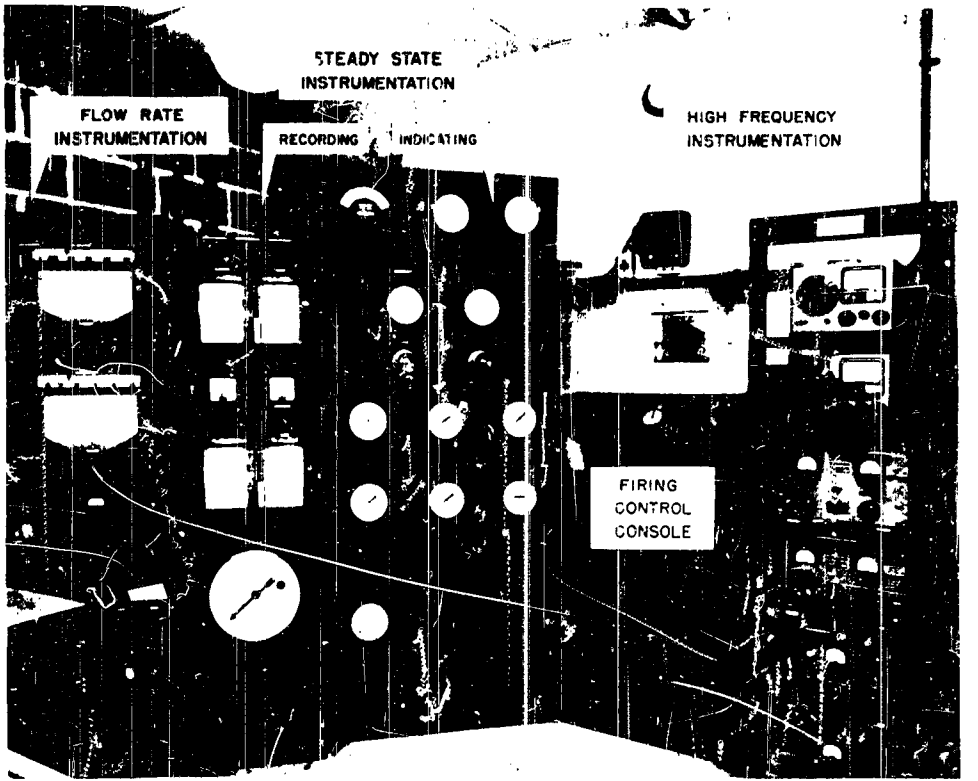

Fig.26 Apparatus for Operating the Rocket Motor

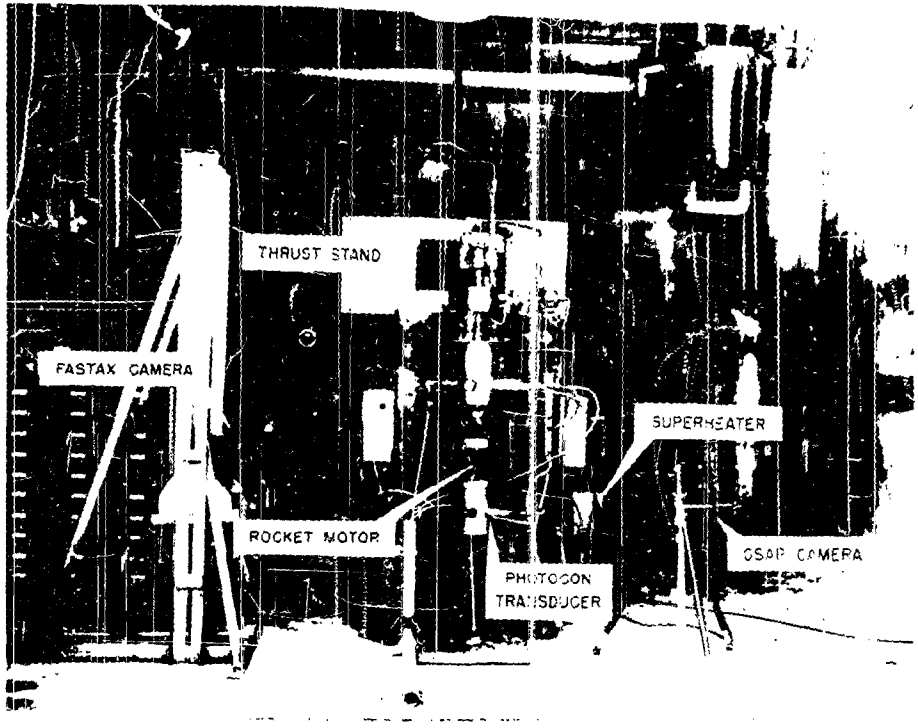

Fig. 27 Rocket Motor Apparatus

means of the latter system the air entered the cell at a constant pressure of 550 psig; the pressure was controlled by a preset Grove "Powreactor Dome" Pressure Regulator (Type RBX 204-02). The pressure of the air supplied to the rocket motor was regulated to the required value, that which would give the required flow rate, by means of a second pressure regulator (Type RBX204-015, externally loaded); the outlet pressure of the latter regulator was set by means of an Atlas reducing and relief valve. The air flow rate was metered by a sharp-edged orifice plate in conjunction with a differential pressure transducer (Wiancko Model P 1203), the output of the latter was recorded on an automatic balancing potentiometer (Minneapolis Honeywell Model 160632-XX-C1). From the orifice plate the air flowed through a bipropellant valve (taken from an Aerojet 38ALDM-1500 JATO unit) to the injector. A safety valve was installed in the air line and was set to limit the maximum pressure to 600 psig.

4(b). Fuel Supply System. The fuels used in the investigation with the exception of propane were supplied from compressed gas bottles. The methane used was commercial grade (93.0 per cent purity), the ethane was research grade (95.0 per cent minimum purity), and the ethylene was research grade (99.5 per cent minimum purity). The methane was supplied at 1800 psig, the ethane at 528 psig, and the ethylene at 1200 psig (each pressure at 70°F). The fuel from the supply cylinder entered the test cell at cylinder pressure and was reduced to a pressure of approximately 550 psig by a preset Grove "Powreactor Dome" Pressure Regulator (Type RBX 204-015). The line pressure of the fuel supplied to the rocket motor was regulated to give the desired flow

rate, an externally loaded Grove "Powreactor Dome" Pressure Regulator (Type WB 206-04) being employed for that purpose. The downstream pressure was regulated to the desired value by means of an Atlas reducing and relief valve. Downstream from the afore-mentioned Grove Regulator the fuel flowed through a sharp-edged orifice plate for metering its flow rate. The differential pressure across the orifice plate was measured by means of a Wianeko differential pressure transducer (Model P120?). From the orifice plate the fuel flowed through the bipropellant valve to the injector.

The propane was transferred from a commercial low pressure bottle illustrated in Fig. 28, to an AISI, Type 347, stainless steel spherical tank which was hydrostatically tested to 1500 psig. The level of the liquid propane inside the stainless steel tank was indicated by means of a sight glass. The stainless steel tank was immersed in an open tank (see Fig. 28) containing a mixture of ethylene glycol and water having a freezing point of $0^{\circ}F$. The water-glycol mixture was heated to a temperature of $170^{\circ}F$ by four electrical immersion heaters (Model TC-4034-230V) made by the E. L. Wiegand Company. At a temperature of $170^{\circ}F$ the propane in the stainless steel tank becomes a saturated liquid at a pressure of 425 psia. When that pressure is reached, a pressure switch (Mercoid Model DA-24) installed in the propane line in the test cell opens an electric circuit to a coil of a 220 volt 90 ampere relay (Allen Bradley Model 70200A92A) which opens the circuit of the four immersion heaters. When the pressure in the propane tank drops to 385 psia, the circuit to the relay coil is closed by the pressure switch which in turn closes the electric circuit for the immersion heaters. Figure 29

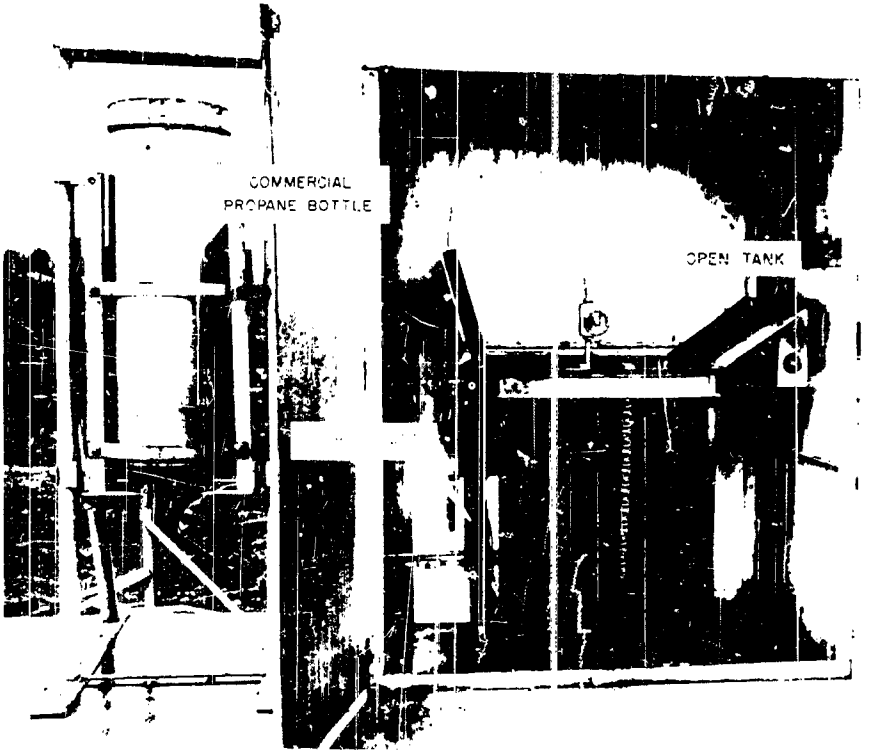

Fig.28 Propane Supply System

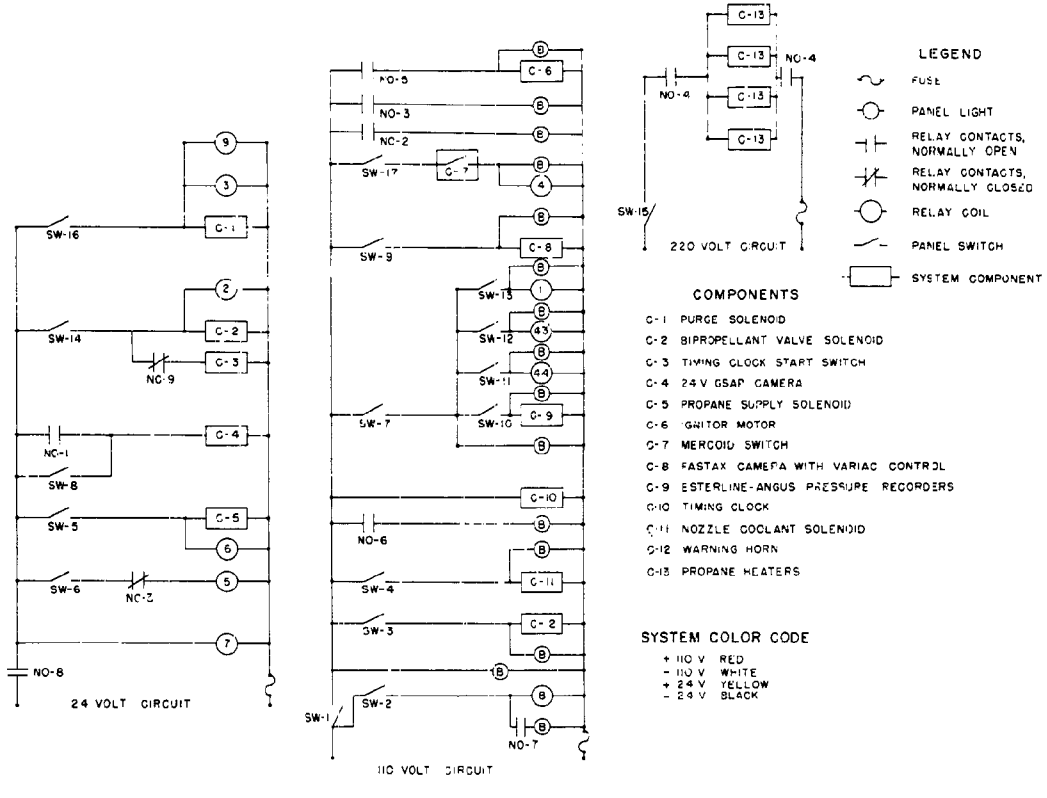

Fig. 29 Schematic Diagram of the Electrical System

is a schematic drawing illustrating the operation of the afore-mentioned relay and immersion heaters.

The propane was supplied to the test cell at a pressure somewhere between 385 and 425 psia. It was discharged from the top of the high pressure stainless steel supply tank, so the propane left the tank in the vapor phase. The line pressure of the propane vapor supplied to the rocket motor was regulated in the same manner as described for methane, ethane, and ethylene. A superheater was installed upstream of the orifice plate in order to insure that the propane was in the superheated vapor state before passing through the orifice.

A safety valve was installed on the high pressure propane tank; the latter was set at 575 psig.

5. Ignition System. The fuel-air mixture fed to the rocket motor combustion chamber was ignited by an automotive type spark plug, which was energized by a magneto (taken from an Allison V1710 engine) driven by a one-quarter horsepower electric motor; the latter was operated remotely from the firing console in the control room.

6. Research Rocket Motor. Figure 30 presents a cross-sectional drawing of the research rocket motor. The internal diameter of the combustion chamber is 3 3/8 inches and its length is determined by the number of sections employed. None of the sections of the combustion chamber were cooled.

7. Mixing Chamber. Figure 31 illustrates the mixing chamber and injector employed in the investigation. The fuel and air entered the mixing chamber through concentric holes: the fuel entered through the central hole and the air through the annulus surrounding that hole. The

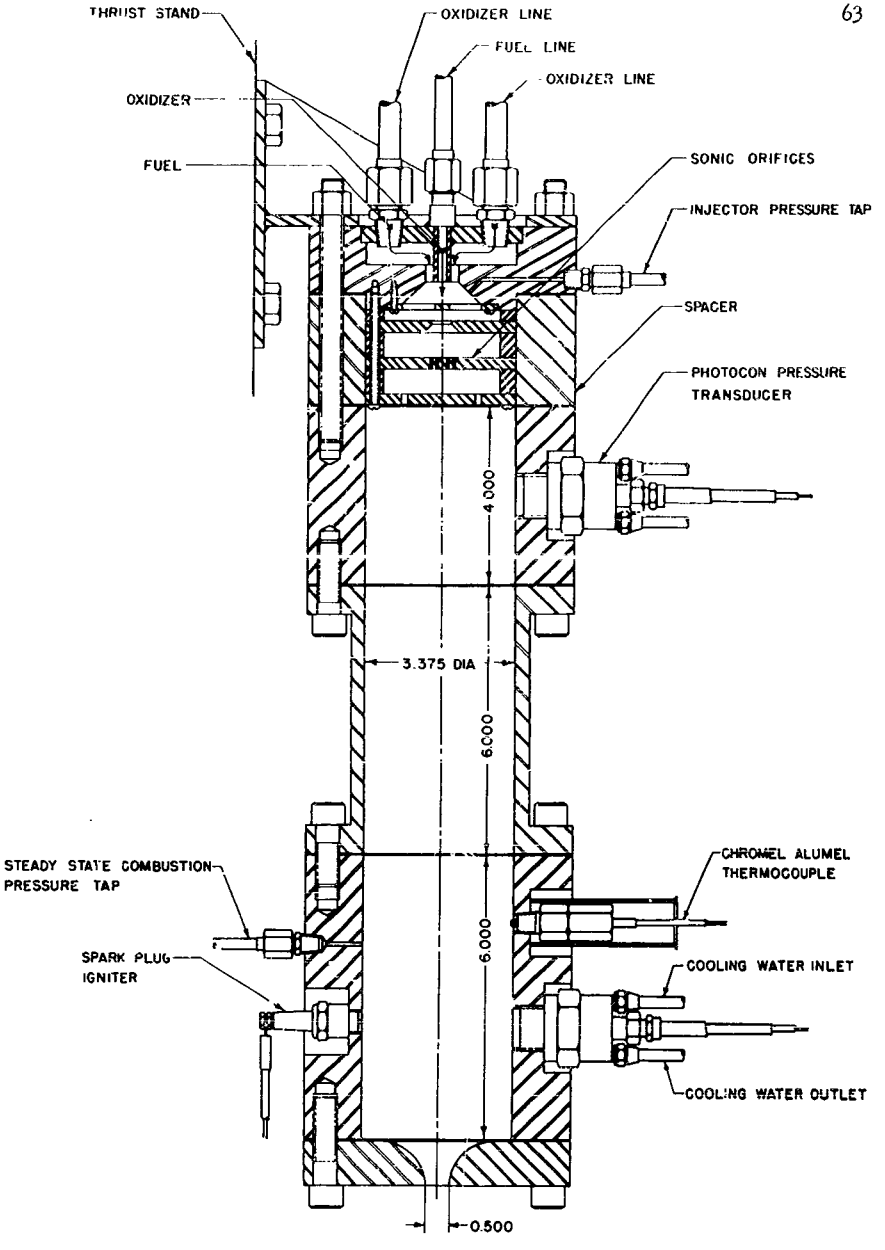

Fig30 Research Rocket Motor

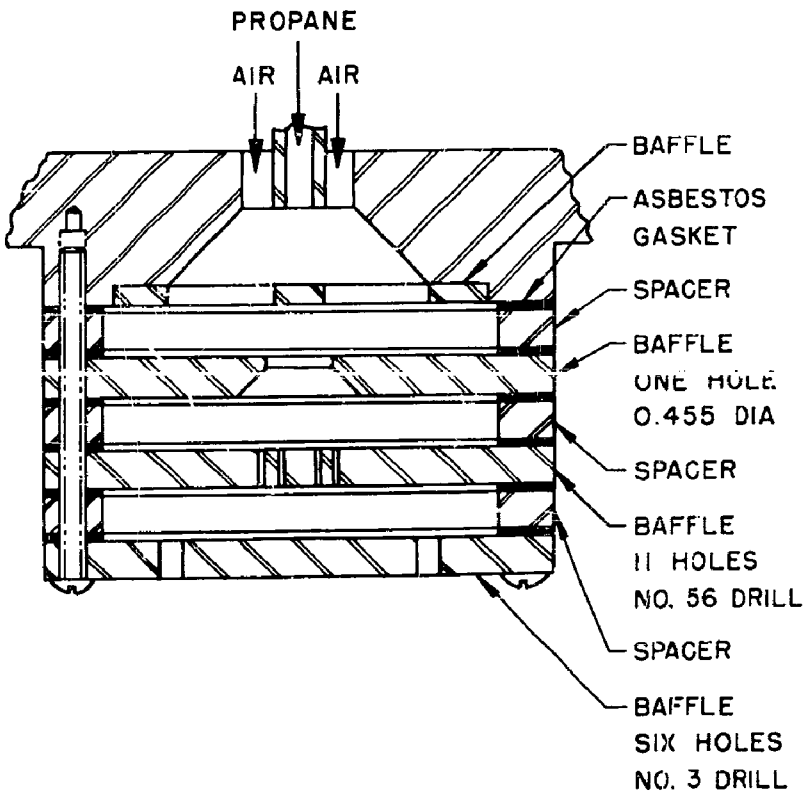

Fig. 31 Injector for High Frequency Experiments

fuel-air mixture then flowed through baffles in the mixing chamber wherein it was thoroughly mixed. The mixing chamber and injection system were designed to operate with a pressure drop of approximately 150 psi so that any tendency for low frequency combustion oscillations to occur would be suppressed.

8. Combustion Chamber. The combustion chamber was assembled from mild steel tubular sections illustrated in Fig. 30. There were four different types of sections. The first type was a thin-walled, uncooled section, six inches long, having no provision for installing high frequency pressure instrumentation. The second type was a heavy-walled uncooled section 4 inches long; it had four holes tapped in the side for installing four high frequency pressure transducers. The third type of section was a heavy-walled uncooled section 6 inches long, which had four tapped holes: one for the spark plug, one for the thermocouple, one for the steady-state combustion pressure tap, and one for a high frequency pressure transducer. The fourth type of section consisted of a group of three spacing rings of 1 inch, 2 inch, and 3 inch lengths whose purpose was to provide a means of varying the length of the combustion chamber from 6 inches to 16 inches in one inch increments. The spacing rings contained no instrumentation.

A fourth spacing ring shown in Fig. 30 was used to sheath the injector.

9. Exhaust Nozzle. The nozzles employed in the investigation are shown in Fig. 4. The one-inch length nozzle was used in the mean combustion pressure-equivalence ratio tests, and the one, two, and four-inch nozzles were used in the nozzle configuration tests.

Instrumentation and Measurements

1. Pressure Instrumentation The instrumentation for measuring pressure can be subdivided into two groups: (a) the high frequency instrumentation and (b) the steady-state instrumentation.

(a) High Frequency Instrumentation. This instrumentation comprised four individual channels of a water-cooled capacitance type pressure transducer (Photocon Model M-30 and 342) and the associated electrical equipment (Dynagage Model D.G. 101 and Power Supply PS102) manufactured by Photocon Research Products). The transducers are illustrated in Fig. 32.

Since the Photocon transducers and electrical equipment were to be employed for measuring rapidly fluctuating pressures, the characteristics of the transducer under such conditions were required. A brief discussion of the method in which the transducers were dynamically calibrated may be found in Reference 1. Figure 33 presents the dynamic response of the Photocon Model M-30 transducers. The outputs of the Photocon transducers were recorded on a six-channel, cathode ray oscillograph (Hathaway Model SC-16B).

The Photocon transducers were statically calibrated before each experiment.

Water cooling was used during the calibration if the transducers were to be water-cooled during the run. The calibration pressure was recorded on the same oscillograph record on which the test pressures were recorded.

(b) The Steady-State Instrumentation. This instrumentation consisted of indicating Bourdon type pressure gages and recording Bourdon tube

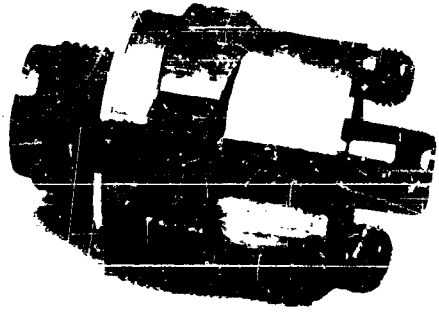

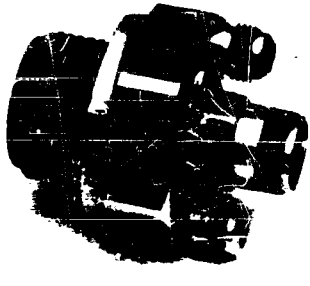

Fig. 32 Photocon Pressure Transducers

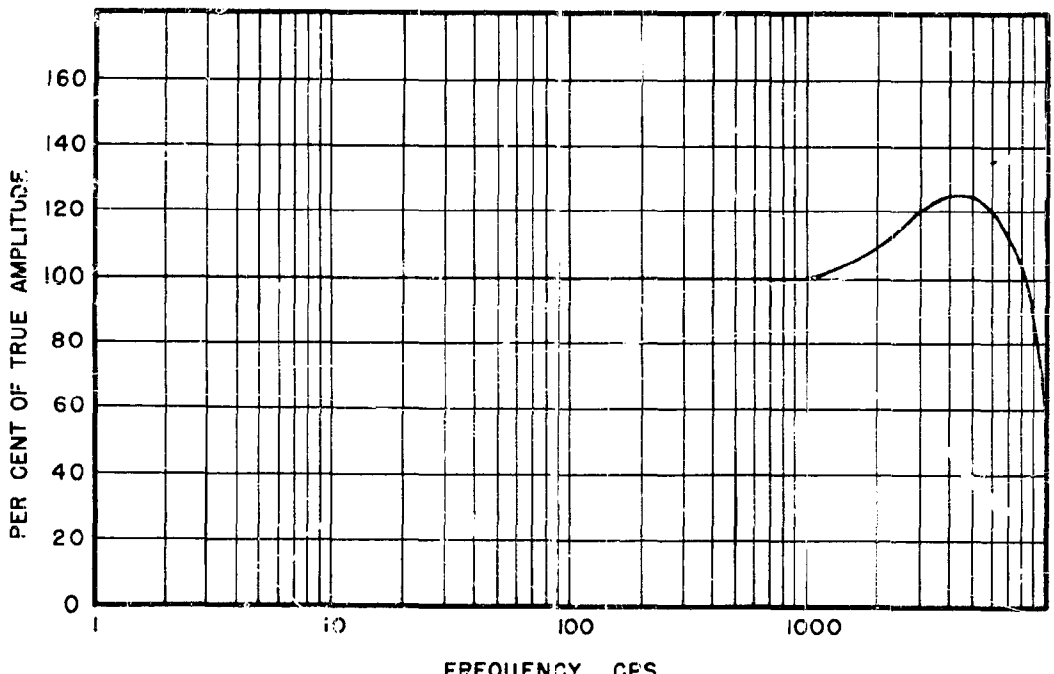

Fig. 33 Dynamic Response of Photocon M-30 Transducer

pressure gages. The recording Bourdon tube pressure gages consisted of four Esterline-Angus Model AW units. The fuel line pressure, the air line pressure, injection pressure, and steady-state combustion pressure were recorded on the above units. The indicating Bourdon tube pressure gages (Marsh Model 103) indicated the following pressures: air line loader pressure, fuel line loader pressure, air line pressure, fuel line pressure, air line pressure outside cell, regulated fuel supply pressure, and air manifold pressure.

2. Propellant Flow Instrumentation and Measurements. Instantaneous flow rates were measured by means of sharp-edged orifices in conjunction with reluctance-type differential pressure transducers. The electrical output from each differential pressure transducer was recorded by an automatic balancing, continuous recording potentiometer. The discharge coefficient for each orifice was determined by calibrating it with water. Since gases were employed as the propellants, the densities were determined from the pressure and temperature measurements made upstream from each orifice plate. The upstream orifice pressures were recorded on the Esterline-Angus units mentioned previously, and the upstream orifice temperatures were indicated on Simplytrol millivoltmeters (Model 351).

APPENDIX C

HEAT-RELEASE RATES OF THE PROPELLANTS

The rate at which two gaseous species react is governed by the frequency at which collisions occur between the molecules of the species and by the proportion of these collisions which produce reaction. The number of collisions which are productive is proportional to $e^{-\frac{E}{RT_f}}$, where E is the activation energy, R the gas constant, and T_f the flame temperature.

The oxidation of a hydrocarbon has been shown to be a chain reaction completed after a large number of collisions between molecules of many intermediate species. It may, however, be supposed that one reaction in the chain is more difficult than the others and that it is this reaction that predominantly controls the rate at which the reaction takes place (9). It may also be assumed that the concentrations of the two species participating in this link are themselves proportional to the concentrations of unburnt fuel and oxygen respectively. This leads to an expression of the form

$$Q = Kp^2 T^{3/2} C_f C_o e^{-\frac{E}{RT}} \qquad (1)$$

where Q is the heat-release rate per unit volume; K is a collision frequency constant; T and p are the local mixture temperature and pressure; and C_f and C_o are the local concentrations of fuel and oxidizer.

A study of equation 1 reveals that the heat-release rate increases as the local mixture pressure and temperature are increased. Since the local mixture pressure increases as the combustion pressure increases, Q also increases with the combustion pressure.

It is convenient to express the temperature and the local concentrations in terms of the over-all fuel/air ratio f, the proportion of fuel remaining unburnt ϵ, and the adiabatic flame temperature T_f. Equation 1 becomes

$$Q = K' \epsilon \left[1 - (1 - \epsilon) f/f^* \right] p^2 \left(T_f - \frac{\epsilon H}{C_p}\right)^{3/2} e^{\left[-\frac{E}{R(T_f - \frac{\epsilon H}{C_p})} \right]} \qquad (2)$$

where

K' is a constant.

f^* is the stoichiometric fuel/air ratio.

H is the calorific value of the combustible mixture.

C_p is the mean specific heat between T and T_f.

Although no data are available for depicting the relationship between the heat-release rates of the afore-mentioned propellants, it is believed that burning velocity measurements for the propellants may be employed in a comparison of the heat-release rates.

For example, nearly all of the theoretical equations (15) for normal burning velocity can ultimately be reduced to the form

$$S^2 = FW \qquad (3)$$

where

S is the normal burning velocity.

F a function of the transport properties of the system, including the diffusion coefficient, the thermal conductivity, viscosity, etc.

W the reaction rate,

Equation 3 can be rewritten

$$S = \left(FA\, e^{-\frac{E}{RT_f}} \right)^{1/2} \qquad (4)$$

where A is the Arrhenius constant.

Since the premixed gases used in the investigations are comprised mostly of air, the function (F) of the transport properties of the system becomes essentially the same for all the propellants used. Thus it is necessary to consider only the differences in burning velocity of the propellants when comparing the propellant reaction rates (or heat-release rates).

Figure 24 illustrates qualitatively the variation of heat-release rate with equivalence ratio for the propellants methane and air, ethane and air, and ethylene and air. Figure 24 is based upon data for the burning velocities of the propellants (10).

Table 1 (Appendix E) presents the dependence of the burning velocity upon initial mixture temperature and pressure for the propellants.

APPENDIX D

PROCEDURE FOR CONDUCTING A ROCKET MOTOR RUN

The general procedure followed in conducting a rocket motor run involved the following.

(1) Selecting the combustion chamber configuration.

(2) Selecting the propellants.

(3) Selecting the instrumentation to be employed.

(4) Calibrating the pressure transducers.

(5) Operation

1. Selecting the Combustion Chamber Configuration. The length of the combustion chamber was altered by changing the length of the tubular sections between the injector and the nozzle. Various lengths ranging from 6 to 28 inches in one-inch increments were available (see Appendix B). Three different exhaust nozzles were available, as described in Appendix B, having a throat diameter of one-half inch and different convergence angles.

2. Selecting the Propellants. The gaseous propellants (methane and air, ethane and air, ethylene and air, and propane and air) were used in the series of experiments concerned with the steady-state combustion pressure and equivalence ratio and the length of combustion chamber. Methane and air were utilized in the nozzle configuration experiments.

For each length of combustion chamber a rocket motor run was made for each of the three propellant combinations.

3. Selecting the Instrumentation to Be Employed. The previously selected combustion chamber configuration determined the number of high frequency pressure transducers to be employed. The steady-state combustion pressure-equivalence ratio and the nozzle configuration experiments utilized four Photocon transducers and the length of combustion chamber experiments utilized one Photocon. The location of the Photocons was described previously.

In addition, measurements were made of the pertinent variables for determining the air flow rate, fuel flow rate, the injector pressure, and the steady-state combustion pressure.

4. Calibrating the Pressure Transducers. A maximum of six pressure transducers were employed in any one rocket motor run. Two of them were differential pressure transducers (Wiancko) employed for measuring the propellant flow rates, the remaining four were high frequency pressure transducers (Photocon). All of the pressure transducers were calibrated before each rocket motor run. Any pressure transducer that was to operate "water-cooled" during a firing run was water-cooled during its calibration.

APPENDIX E

PROPERTIES OF THE PROPELLANTS

FLAME SPEEDS OF THE PROPELLANTS AT STOICHIOMETRIC

PROPELLANTS	EXPERIMENTAL VALUE OF BURNING VELOCITY $S \frac{cm}{sec}$	PRESSURE DEPENDENCE OF BURNING VELOCITY	TEMPERATURE DEPENDENCE OF BURNING VELOCITY	FLAME TEMPERATURE T_f °K	ACTIVATION ENERGY $E \frac{kcal}{mole}$
METHANE-AIR	38.9	$P^{-\frac{1}{4}}$	$S=8-0.000160T^{2.11}$	2200	26
ETHANE-AIR	44.5	———	———	2'95	26
PROPANE-AIR	44.0	$P^{-\frac{1}{3}}$	$S=10+0.000342T^{2.00}$	2260	26
ETHYLENE-AIR	74.2	$P^{-\frac{1}{3}}$	$S=10-0.00259T^{1.74}$	2340	24

DATA FROM REFERENCES 12,13,14

TABLE I

APPENDIX F

BIBLIOGRAPHY

1. Osborn, J. R., An Experimental Study of Combustion Pressure Oscillations in a Gaseous Bipropellant Rocket Motor, Ph.D. Thesis, Purdue University, June 1957.

2. Osborn, J. R., and Zucrow, M. J., An Unclassified Literature Survey on Combustion Pressure Oscillations In Liquid Propellant Rocket Motors, Jet Propulsion Center, Purdue University, Report No. TM57-1.

3. Barrare, M., and Moutet, A., Low Frequency Combustion Instability in Bipropellant Rocket Motors - Experimental Study, Journal of the American Rocket Society, Vol. 26, No. 1, p. 9, January 1956.

4. Berman, K., and Logan, S. E., Combustion Studies with a Rocket Motor Having a Full-Length Observation Window, Journal of the American Rocket Society, Vol. 22, No. 2, p. 78, March 1952.

5. Berman, K., and Cheney, S. H., Jr., Combustion Studies in Rocket Motors, Journal of the American Rocket Society, Vol. 23, No. 2, p. 89, March 1953.

6. Berman, K., and Cheney, S. H., Jr., Rocket Motor Instability Studies, Journal of the American Rocket Society, Vol. 25, No. 10, p. 513, October 1955.

7. Tischler, A. O., Massa, R. V., and Matler, R. L., An Investigation of High-Frequency Combustion Oscillations in Liquid Propellant Rocket Engines, NACA RM E53B27, June 1953.

8. Mickelsen, W. R., Effect of Standing Transverse Acoustic Oscillations on Fuel-Oxidant Mixing in Cylindrical Combustion Chambers, NACA TN 3983, May 1957.

9. Bragg, S. L., and Holliday, J. B., The Influence of Altitude Operating Conditions on Combustion Chamber Design, AGARD Selected Combustion Problems II, Butterworth's, London, p. 270.

10. Jost, W., Explosion and Combustion Processes in Gases, McGraw Hill Book Co., Inc., New York, 1946, p. 74.

11. Crocco, L., and Cheng, Sin-I, Theory of Combustion Instability in Liquid Propellant Rocket, Monograph 8, AGARD, NATO, Butterworth Scientific Publications, London, 1956.

12. Egerton, Sir Alfred, and Sen, D., Flame Propagation: The Influence of Pressure on the Burning Velocities of Flat Flames, Fourth Symposium (International) on Combustion, Williams & Wilkins Co., 1953.

13. Dugger, G. L., and Simon, D. M., Prediction of Flame Velocities of Hydrocarbon Flames, Fourth Symposium (International) on Combustion, Williams & Wilkins Co., 1953.

14. Dugger, G. L., and Heimel, Sheldon, Flame Speeds of Methane-Air, Propane-Air, and Ethylene-Air Mixtures at Low Initial Temperatures, NACA TN 2624, February, 1952.

15. Fenn, J. B., and Calcote, H. F., Activation Energies in High Temperature Combustion, Fourth Symposium (International) on Combustion, Williams & Wilkins Co., Baltimore, 1953.